

# **X-ray fluorescence analysis**

**A. Somogyi**

**ID22, European Synchrotron Radiation Facility, ESRF, Grenoble France**

## **Outline**

- **What is X-ray fluorescence analysis (XRF)?**
- **Micro-X-ray fluorescence analysis**
- **Application of scanning μ-XRF**
- **X-ray fluorescence tomography and applications**
- **Combination of μ-XRF with other μ-X-ray techniques ( μ-XRD, μ-XANES, μ-tomography)**
- **Conclusion**

## **Collaborators:**

- **J. Susini, M. Salome, R. Baker,  
ID21**
- **B. Golosio, S. Bohic, M.  
Drakopoulos, S. Labouré,  
ID22/ID18F**
- **R. Toucoulou, ID21/ID22**
- **B. Fayard, A. Simionovici(CNRS)**

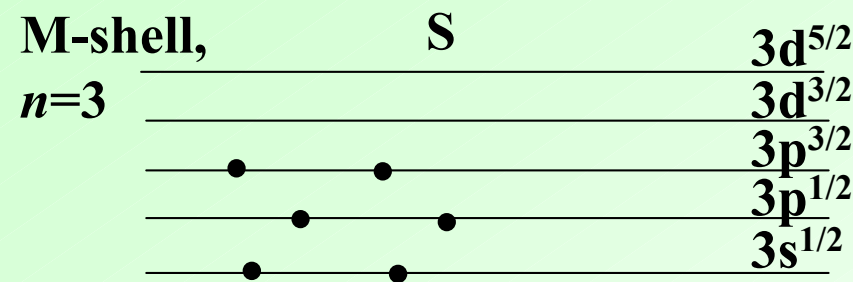
# What is X-ray fluorescence analysis?

X-ray fluorescence spectra:

Originate from a lack of an electron in an inner electron shell

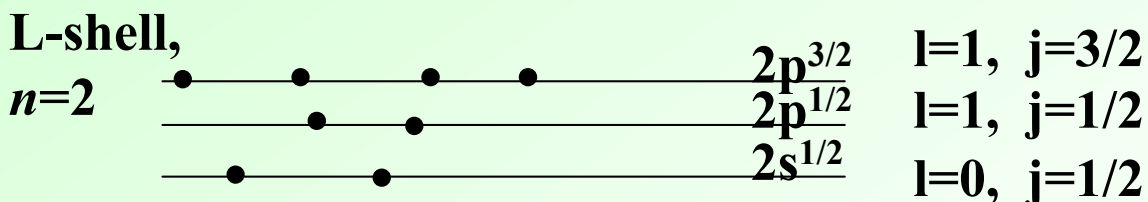
Electron configuration in an atom

- electron states are determined by the  $n, l, m, j$  quantum numbers
- electron shell: specified by the  $n$  principal quantum number
- electron subshell: determined by  $l, j$
- energy of an atomic electron is determined by  $Z, n, l, j$



Pauli exclusion principle

Stable atom: inner electron shells (largest e<sup>-</sup> binding energy) are filled



$l=1, j=3/2$   
 $l=1, j=1/2$   
 $l=0, j=1/2$

closed subshell:  $2j+1 e^-$



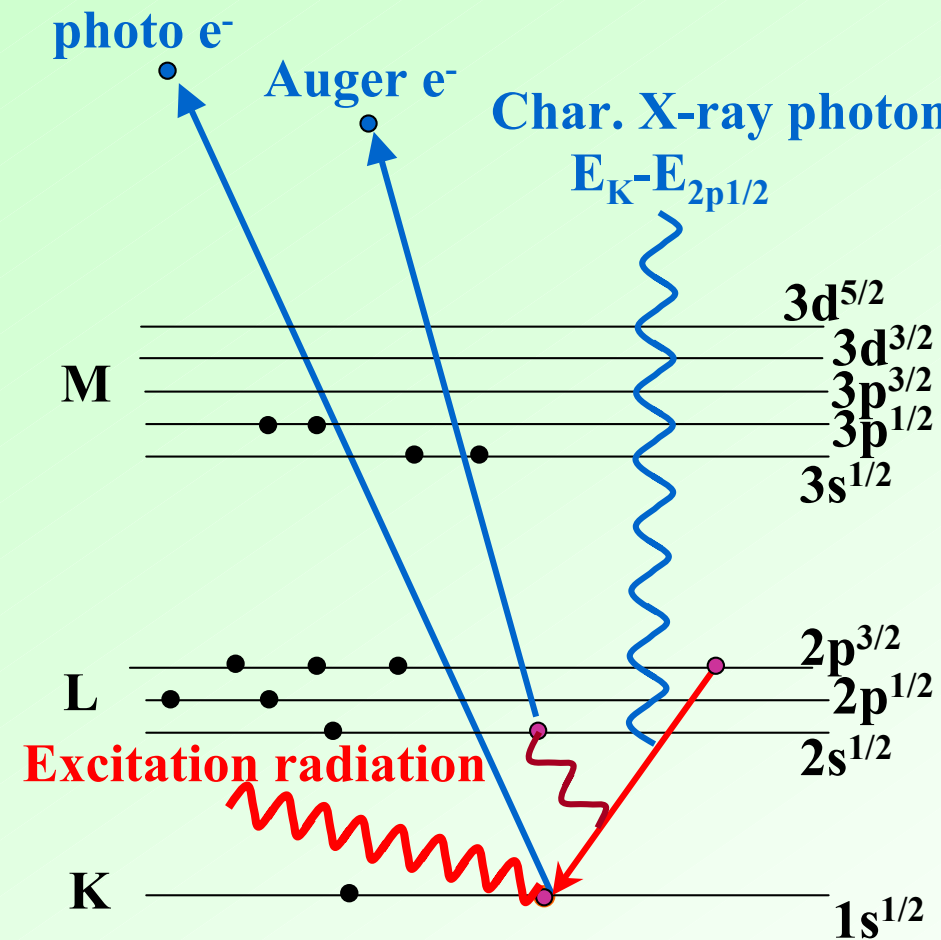
# What is X-ray fluorescence analysis?

Stable state: all the inner shells are filled, till the valence state

Excitation: one electron is removed from one of the inner shells (K, L, ...),  
‘hole’ is created by X-ray photons

Electrons

Protons



Deexcitation by readjustment of the  
electron cloud  
electron transition from outer shells

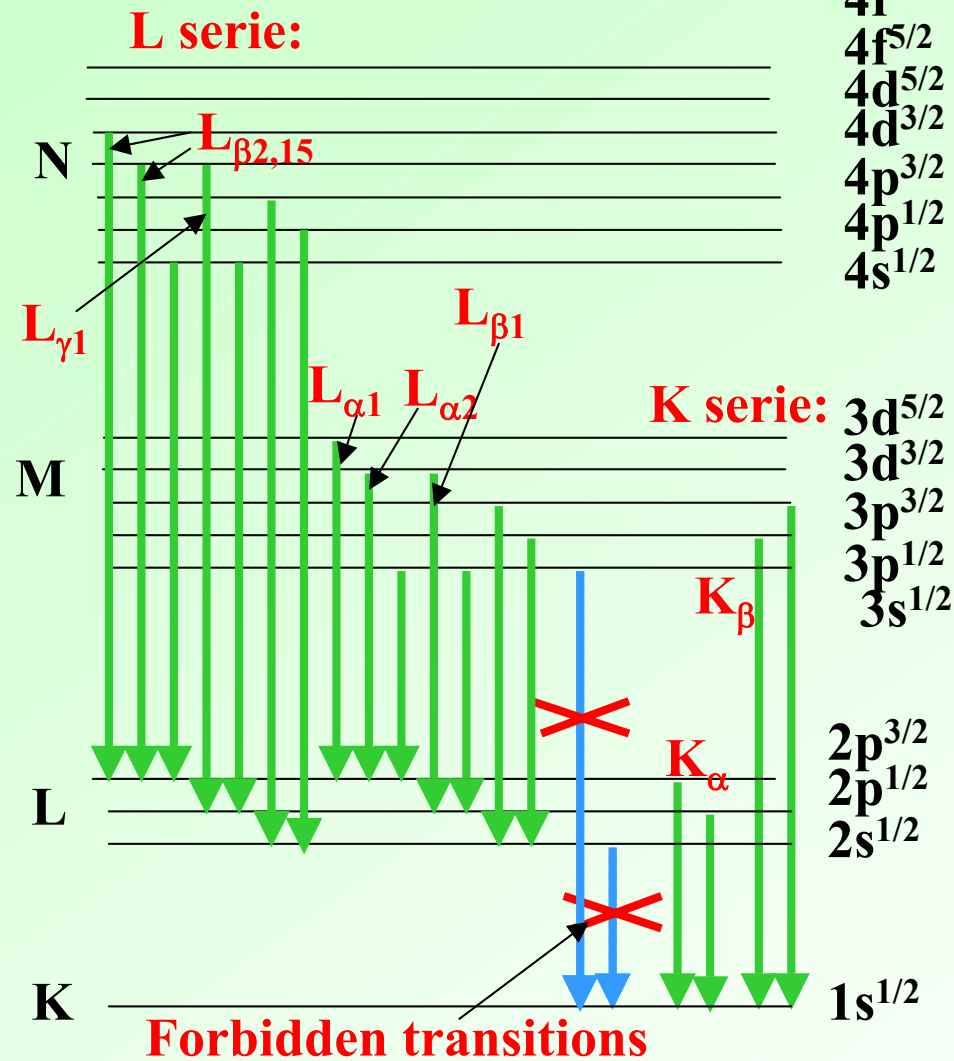
$E_K > E_L !!$

$E_K - E_L$  will be released, e.g. by

Characteristic X-ray photon  
Photoelectrons  
Auger electrons

# How does an X-ray spectrum look like?

## Diagramm lines



$4f^{7/2}$   
 $4f^{5/2}$   
 $4d^{5/2}$   
 $4d^{3/2}$   
 $4p^{3/2}$   
 $4p^{1/2}$   
 $4s^{1/2}$

$3d^{5/2}$   
 $3d^{3/2}$   
 $3p^{3/2}$   
 $3p^{1/2}$   
 $3s^{1/2}$

$2p^{3/2}$   
 $2p^{1/2}$   
 $2s^{1/2}$   
 $1s^{1/2}$

## Electric-dipole selection rules

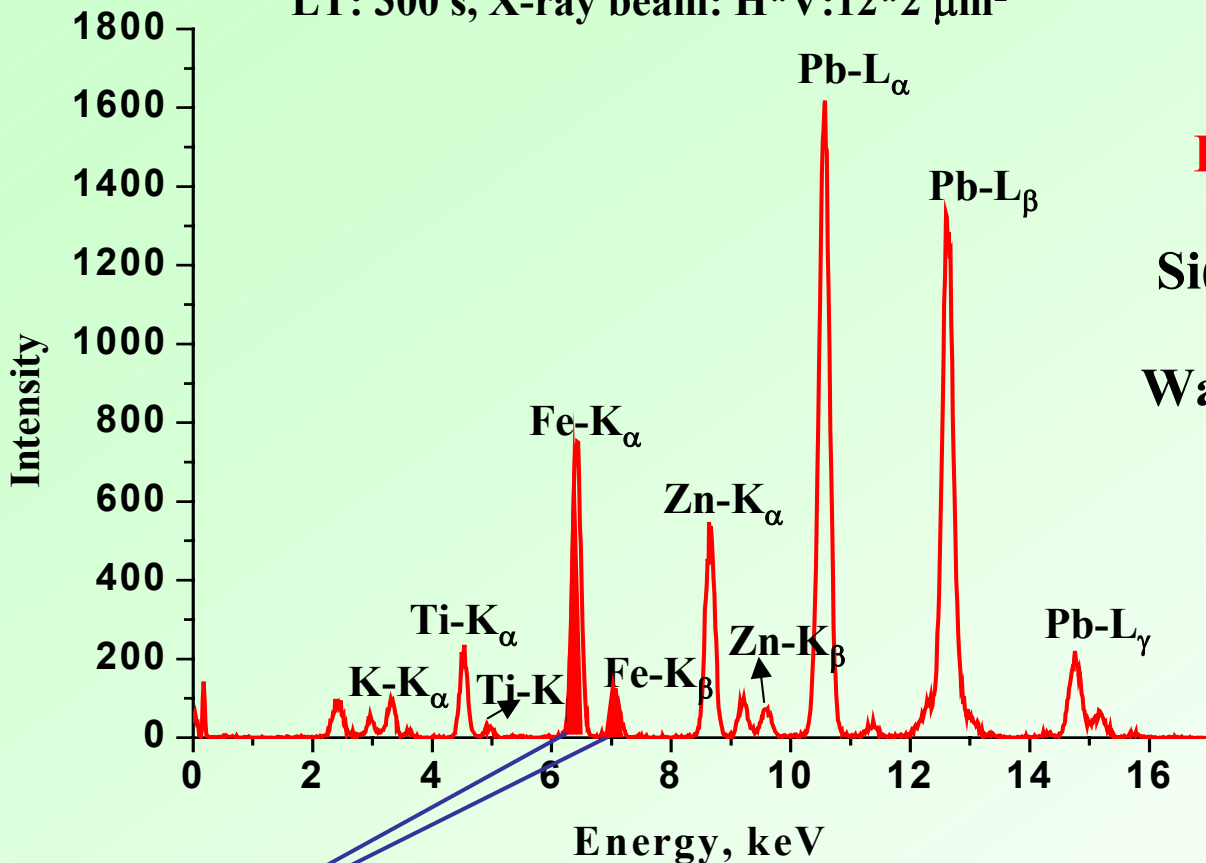
$\Delta n \neq 0$   
 $\Delta l = \pm 1$   
 $\Delta j = 0, \pm 1$

First 4 elements, H, He, Li, Be have **no characteristic X-ray** diagramm lines

New transitions become possible with the filling up of the outer electron shells

# How does an X-ray spectrum look like?

XRF spectrum of thin glass standard SRM1833,  
LT: 300 s, X-ray beam: H\*V:12\*2  $\mu\text{m}^2$



**Detection of XRF spectra:**

Si(Li) solid state spectrometer

Wave-length dispersive crystal  
spectrometer

Energies of the X-ray lines

qualitative analysis

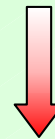
Intensity of a given X-ray line

~number of a given atom in the excited  
volume, quantitative analysis

# What is X-ray fluorescence analysis?

How can we knock out an electron from an inner electron shell?

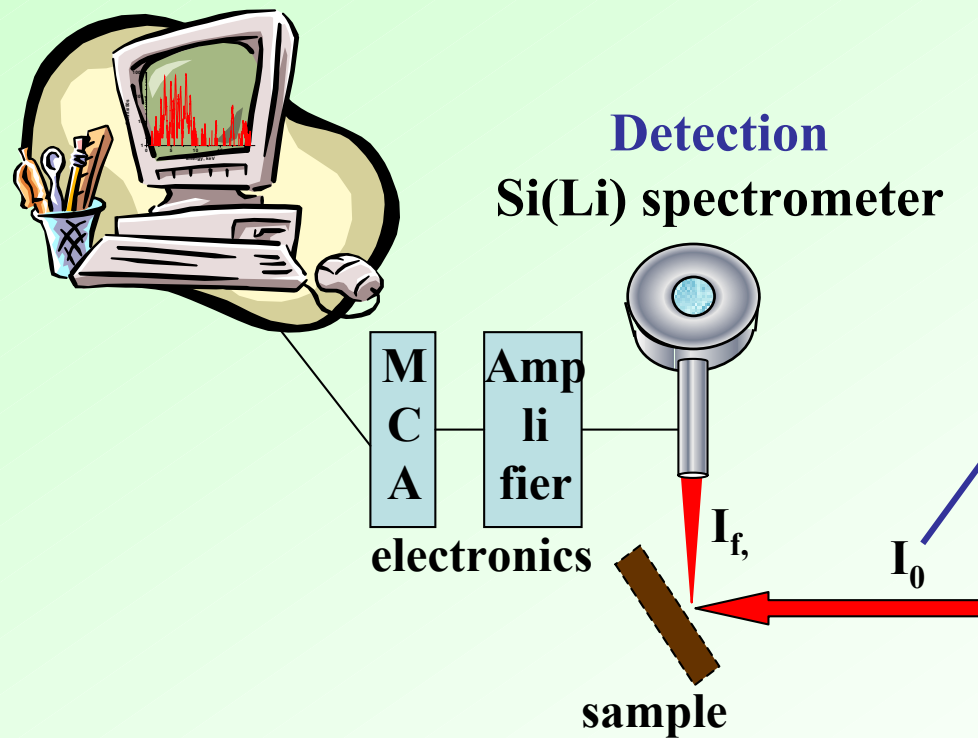
With **X-ray**,  $\gamma$ -ray, electrons, ions with  $E > E_K$  or  $E > E_L$



**X-ray fluorescence analysis:**

Inner  $e^-$  shell excitation by X-rays

Detection of characteristic X-ray photons (X-ray spectra)

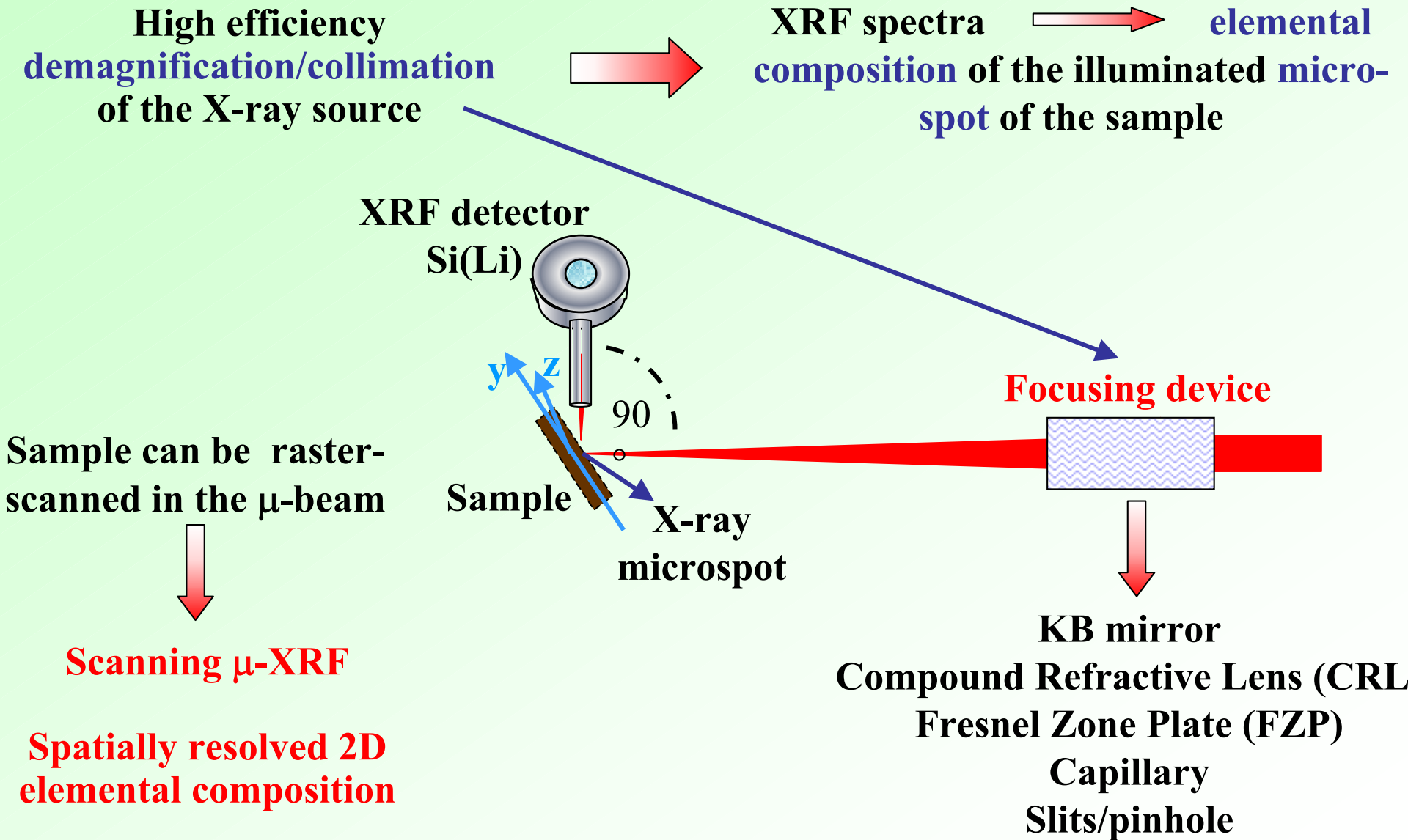


**X-ray excitation sources:**

- X-ray radioisotope
- X-ray tube
- Synchrotron beam

Laser like **X-ray beam** with low divergence and high spectral brilliance

# Micro-X-ray fluorescence spectrometry

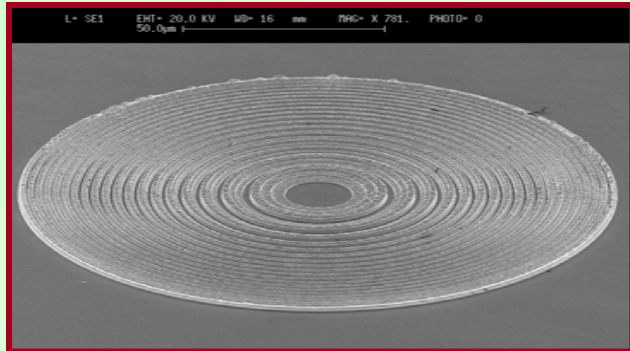


# Micro-X-ray fluorescence spectrometry

## Focusing devices

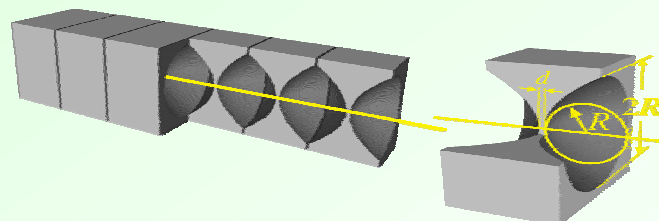
### Fresnel Zone Plates (FZP) Diffractive Optics

- diffraction gratings of increasing linear density
- 50-60 % efficiency
- spot size:  $< 0.1 \times 0.1 \mu\text{m}^2$  (for low E)

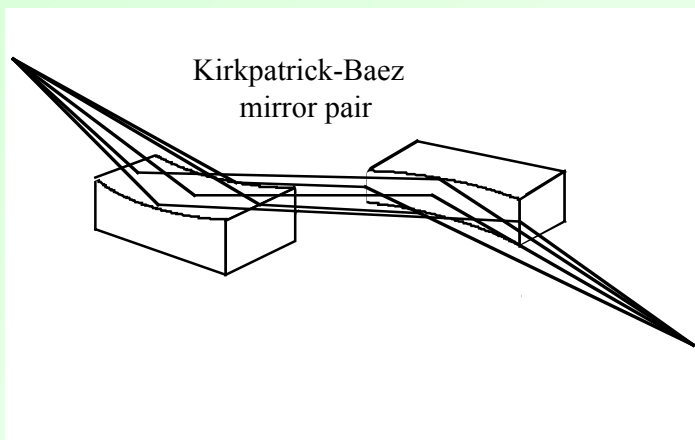


### Compound Refractive Lenses (CRL) Refractive Optics

- parabolic lenses - reduced aberrations
- variable n assemblies: tune f and  $L_2$
- high yield for high E
- spot size:  $\sim 2 \times 12 \mu\text{m}^2$



### Bent mirrors Kirkpatrick-Baez, (KB mirror pair) Reflective optics



- 60-70 % efficiency
- achromaticity
- Multilayer mirror for high energy
- spot size:  $\sim 1 \times 3 \mu\text{m}^2$

# **Synchrotron radiation induced scanning $\mu$ -XRF**

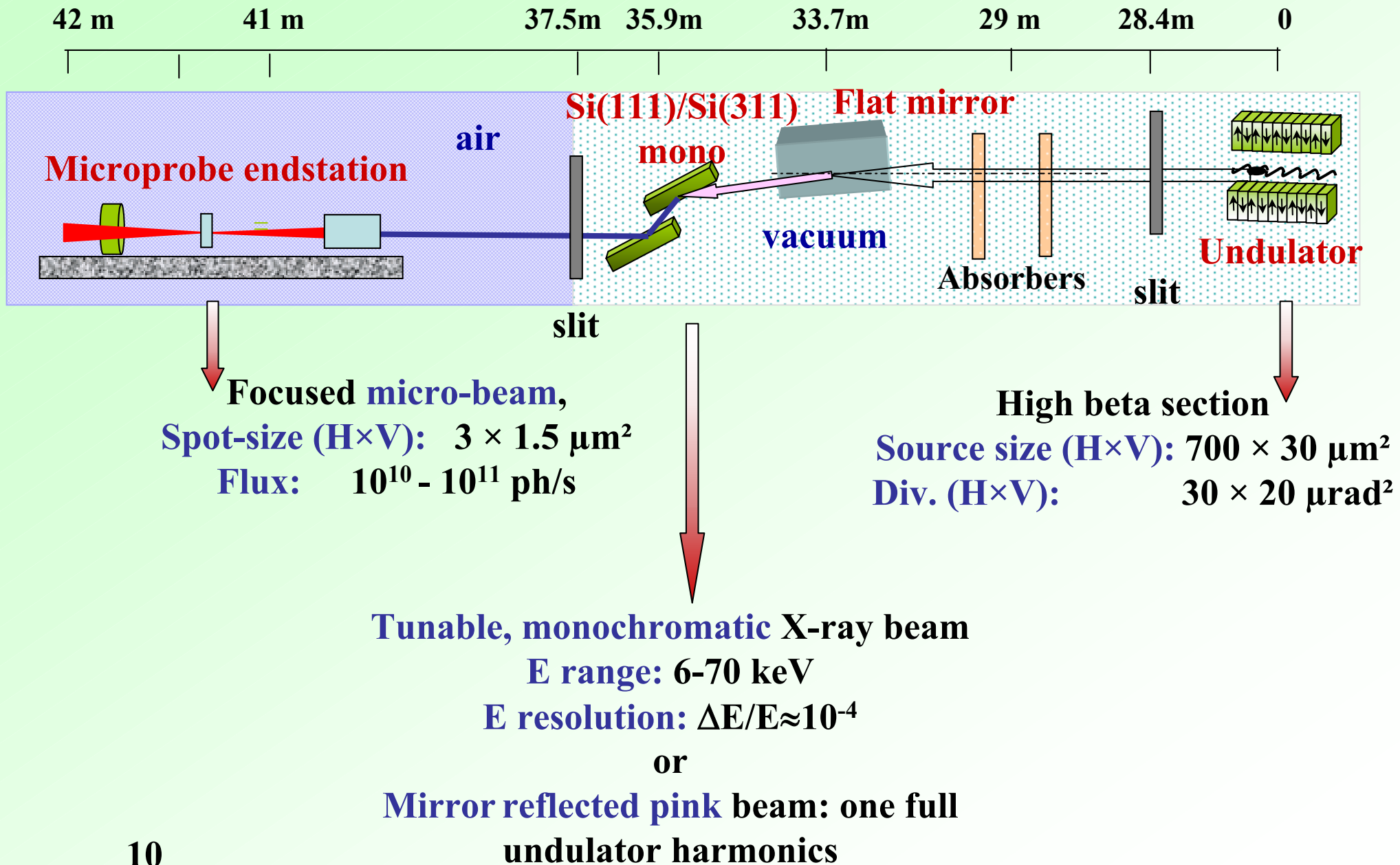
## **ID21, ID22 beam-lines of the European Synchrotron Radiation Facility (ESRF)**

	<b>ID21 X-Ray Microscopy</b>	<b>ID22/ID18F Micro-XRF, Imaging, Diffraction</b>
• Energy range:	<b>2-8 keV</b>	<b>6-70 keV</b>
• Spatial resolution:	<b>0.1 - 1.0 <math>\mu</math>m</b>	<b>1.5 - 3.0 <math>\mu</math> m</b>
• Monochromator:	<b>Si 111 or Si 220</b>	<b>Si 111 or Si 311</b>
• Detection:		<b>parallel multiple detection</b>
• Fluorescence:	<b>HPGe</b>	<b>Si(Li)</b>
• Transmission:	<b>photodiode</b>  <b>operation in air/vacuum</b>	<b>photodiode, ion. chamber</b>  <b>operation in air</b>
• Detectable elements: (by XRF)	<b>Z&lt;26 (Fe) K-lines</b>  <b>Z&lt;64 (Gd) L-lines</b>	<b>14&lt;Z&lt;72 (Hf) K-lines</b>  <b>72&lt;Z L-lines</b>

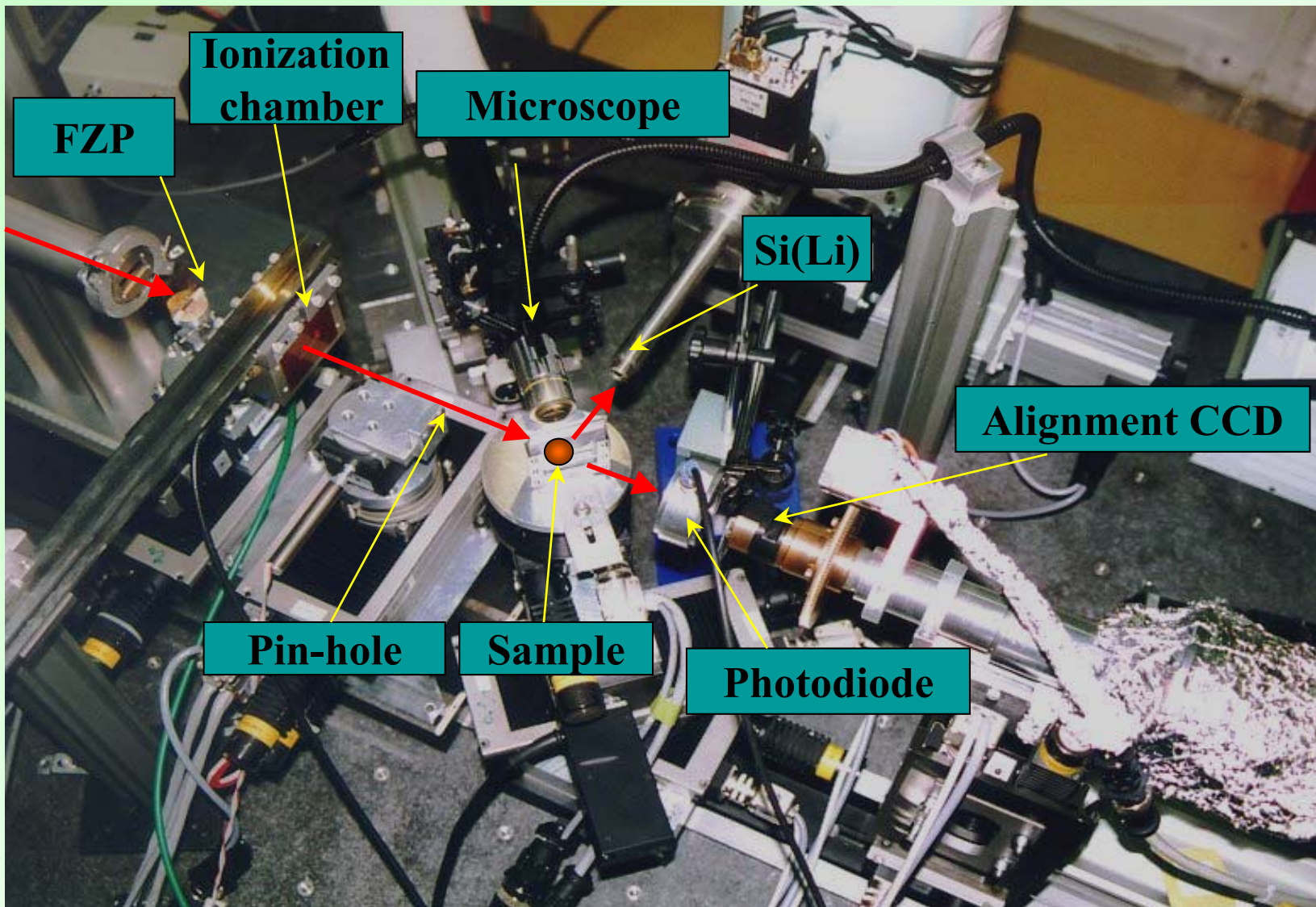
### **Applications:**

**Geochemistry, Biology, Environmental Sciences, Materials Science...**

# Schematic layout of the ID22 beam line and the microprobe end-station

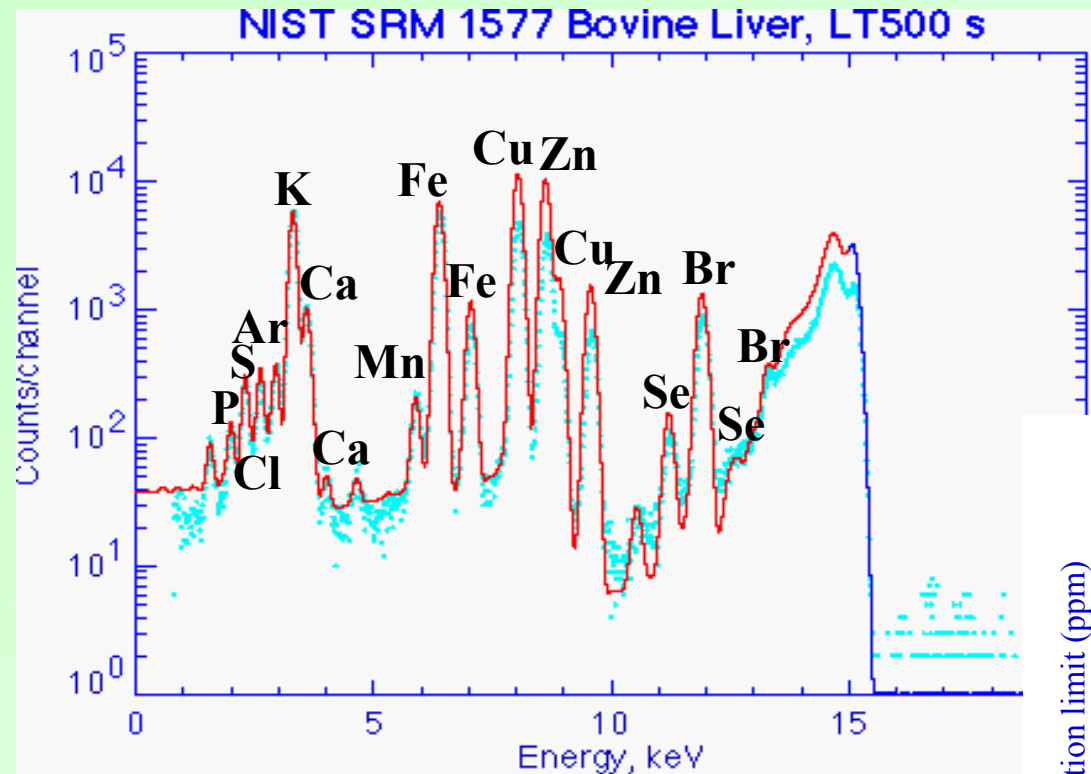


## X-ray microprobe set-up at ID22



# X-ray microprobe set-up at ID22, ESRF

## Minimum limit of detection

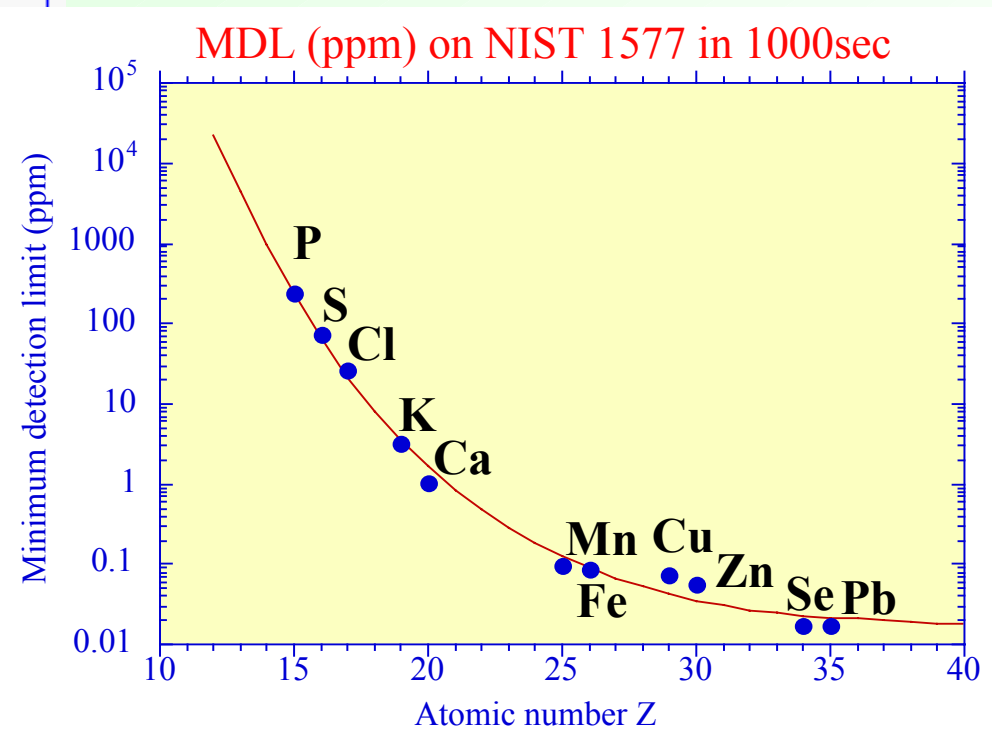


$10^{10}$ - $10^{11}$  photons/s in the focused beam

Detection limit/1000 s:

$\approx 20$  ppb  
 $\approx 0.4$  fg

$E=15$  keV,  $1 \times 5 \mu\text{m}^2$

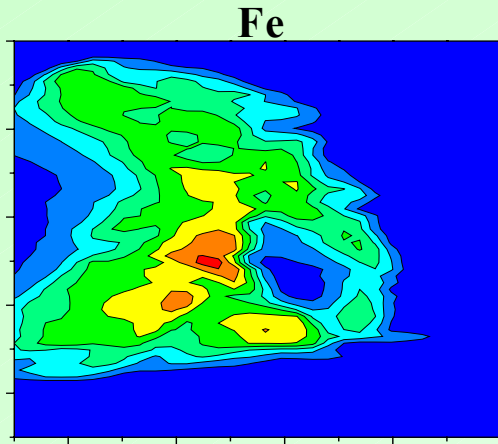


# Scanning micro-XRF, geological applications

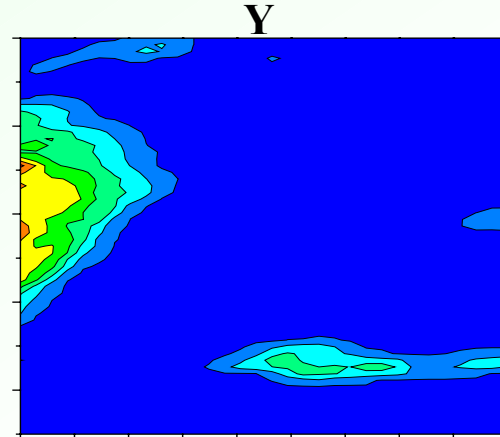
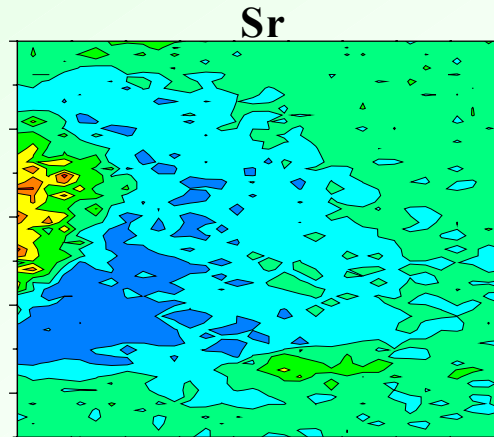
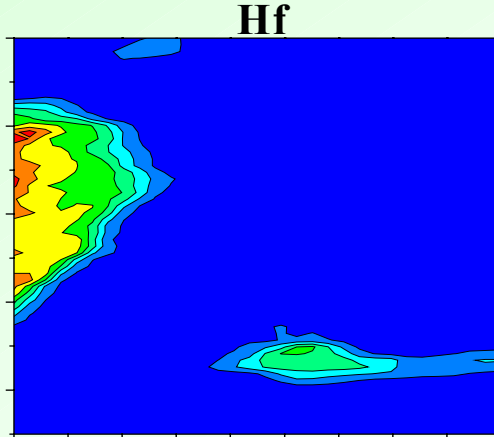
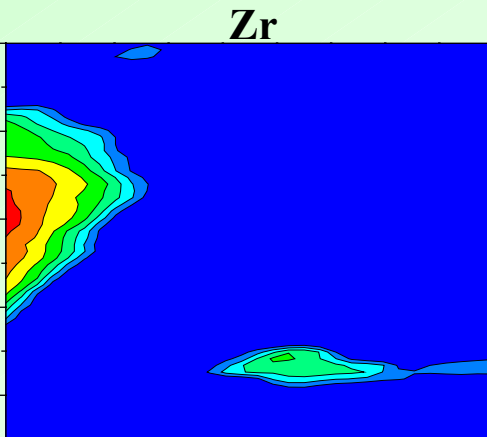
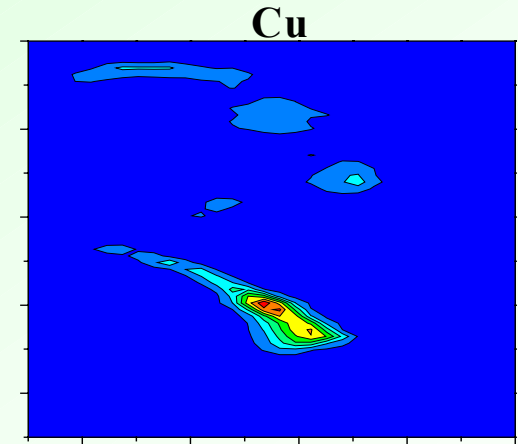
## Inclusions in obsidian

In collaboration: A.Z. Kiss, IBA-ATOMKI, Gy. Szoor, Univ. of Debrecen, Hungary

Flat obsidian slice of ~50  $\mu\text{m}$  thickness, LT:6 s/pixel, spot: H\*V=8\*1.5  $\mu\text{m}^2$ , ID22  
Vinicky, Slovakia



**Obsidian: volcanic glass, inclusions:  
mineral phase of  $\mu\text{m}$  size. Its  
chemical composition is characteristic  
to the geographical source.  
⇒ Distinction of ancient  
archeological obsidian sources  
from e.g Hf/Zr, Y/Sr conc. ratio.**



Combination with other analytical techniques, LA-ICP-MS, SEM-EDAX, PIGE, PIXE,  
optical microscopy

# Scanning micro-XRF, geological applications

## Quantitative mapping of trace elements in fluid inclusions

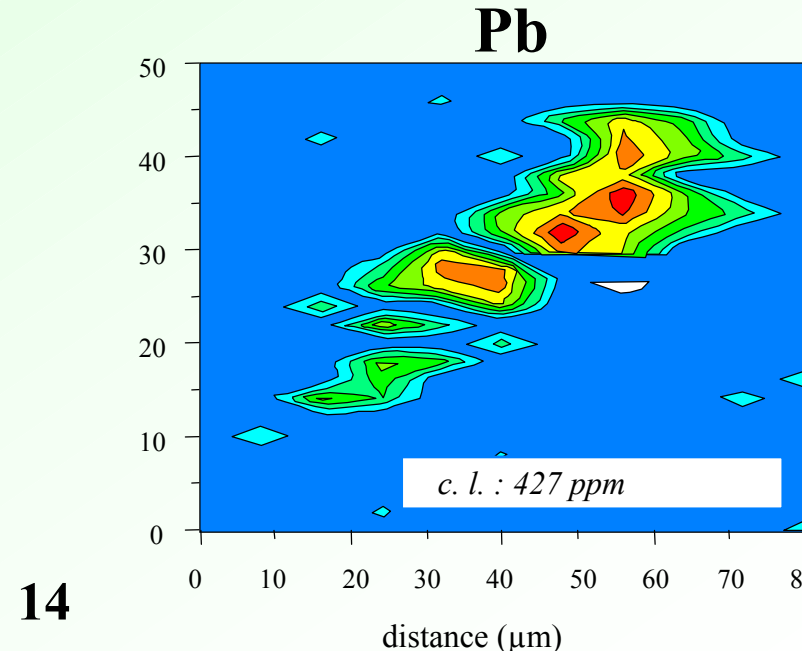
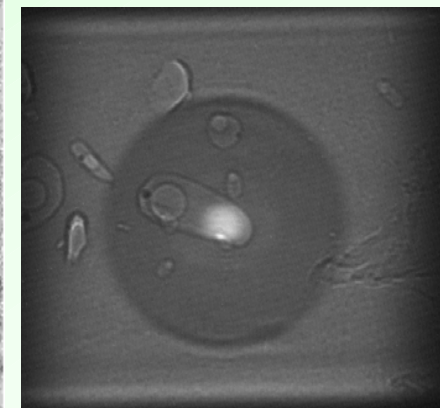
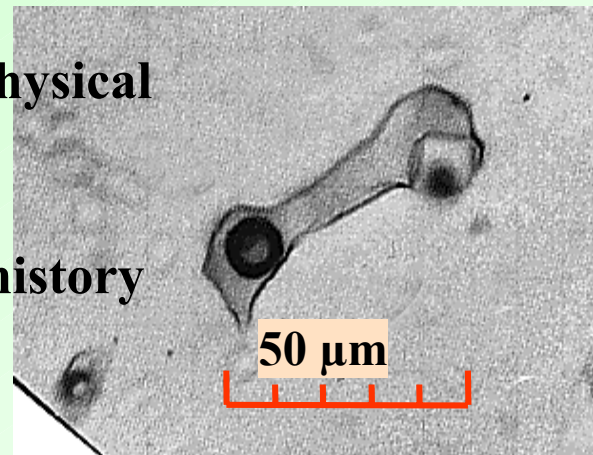
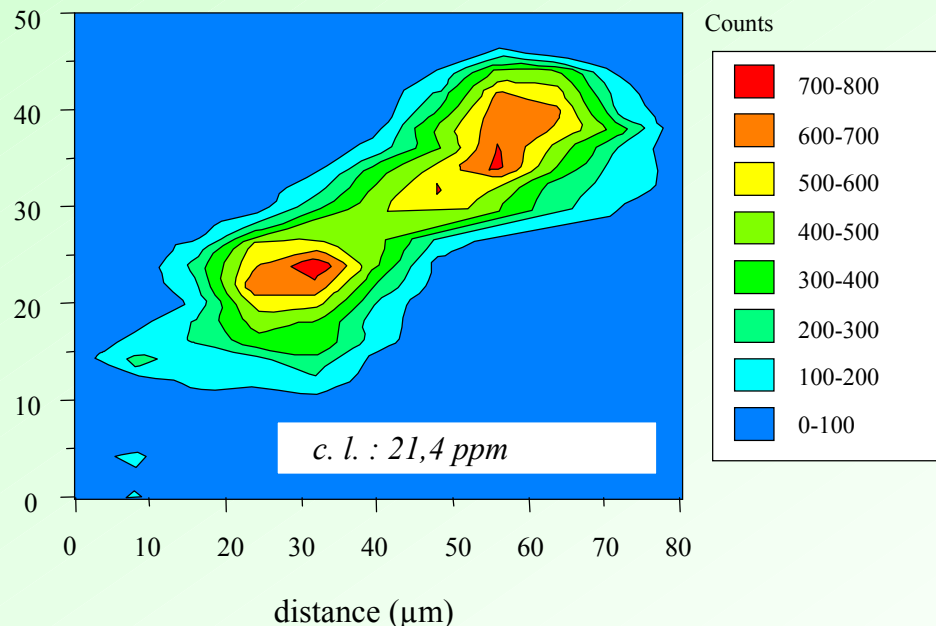
P. Philippot, B. Ménez, Univ. Paris VI, France, A. Simionovici, CNRS, Lyon

Fluid inclusion: preservation of chemical, physical properties of the original parent fluid  
(if closed system)

Unique direct fossil samples of the Earth's history

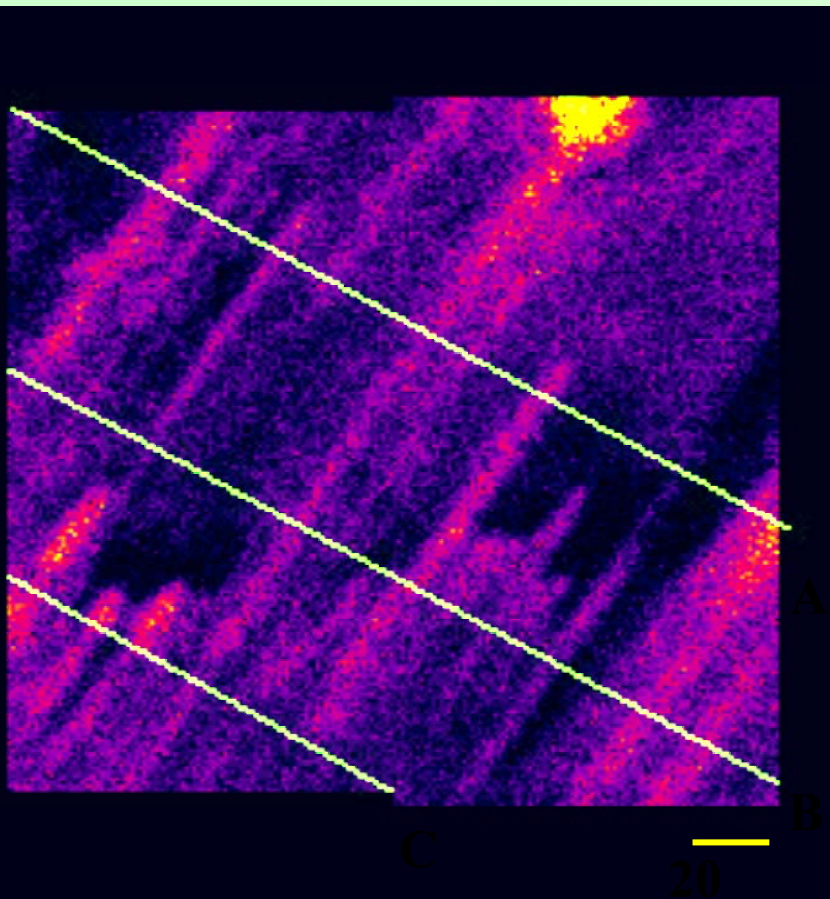
E=12 and 20 keV, (FZP+CRL) focusing  
non-destructive analysis,  $t \approx 5 - 30$  s/pt

Br



# Scanning micro-XRF, geological applications

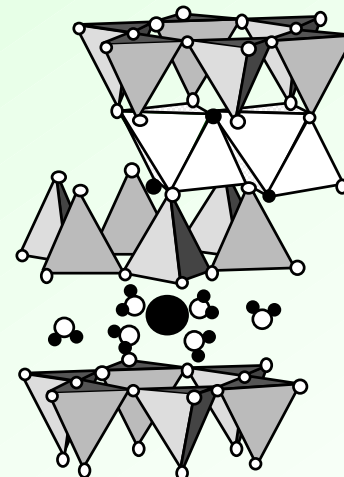
## Oriented Meso-structures in clay gels, ID21



Observation of periodical ordering on length-scales 2 orders of magnitude larger than expected/known before

- Wyoming montmorillonite gel (50g/l), Prepared as hydrated sample (in vacuum)

- Excitation energy 2.5 keV
- Fluorescence yield of Silicon
- Spatial resolution < 1  $\mu\text{m}^2$



- Oxygen
- Hydroxyl
- Water molecules
- Exchangeable cation

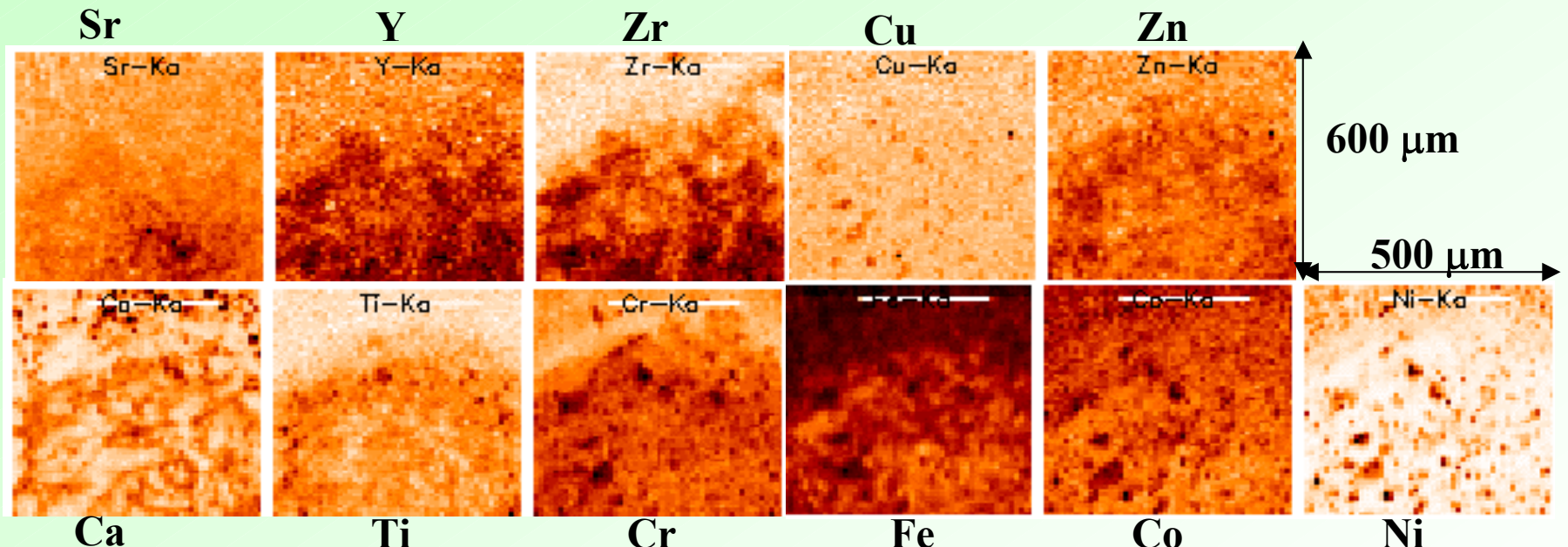


# Scanning micro-XRF, astrochemical applications

## Allende meteorite

In collaboration with F. Adams, K. Janssens, B. Vekemans, L. Vincze Univ. of Antwerp, Belgium

Mapping one part of a chondrule: 50(10  $\mu\text{m}$ )x60(10  $\mu\text{m}$ ), LT/pixel: 10 s, ID18F



Meteorites are the only objects from the early stage of the solar system available for research, carbonaceous chondrites are one of the oldest objects of the solar system.



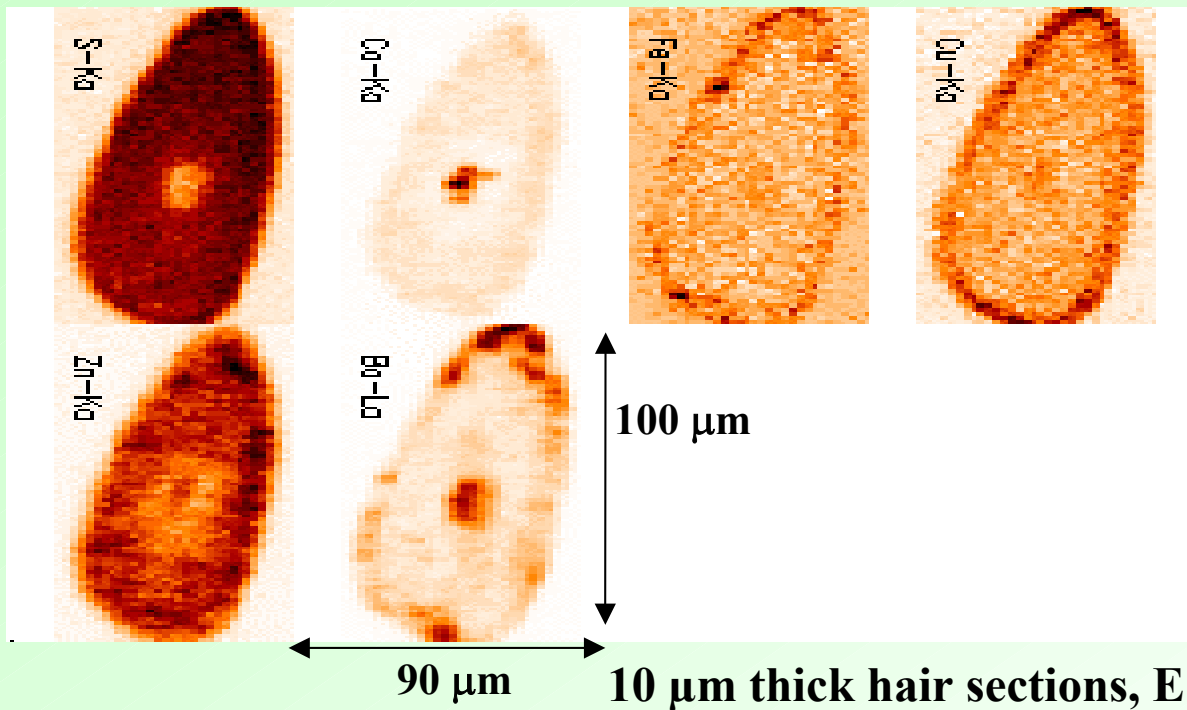
correlations between different elements,

possible formation mechanism of chondrule on the basis of Zn distribution?

# Scanning micro-XRF, biological applications

## XRF mapping of hair sections, ID18F

In collaboration with S. Bohic, ID22, ESRF, France, Y. Duvault: L'Oréal, P. Dumas: LURE, France



### Aim of the study:

Anomalies of elemental distribution: stress? Chemicals?

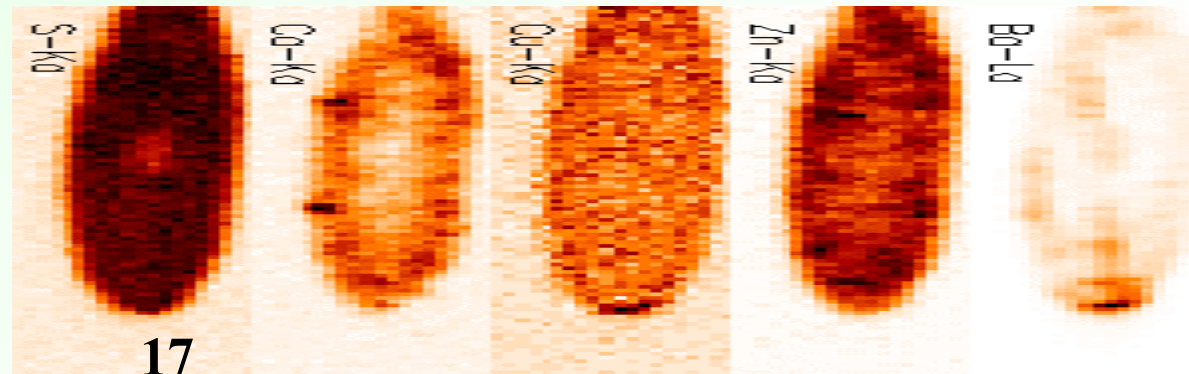
Effect of cosmetics, new developments

Medical diagnostics?

10 μm thick hair sections, E: 17 keV, spot size 2x4 μm<sup>2</sup>, LT:7 s/pixel

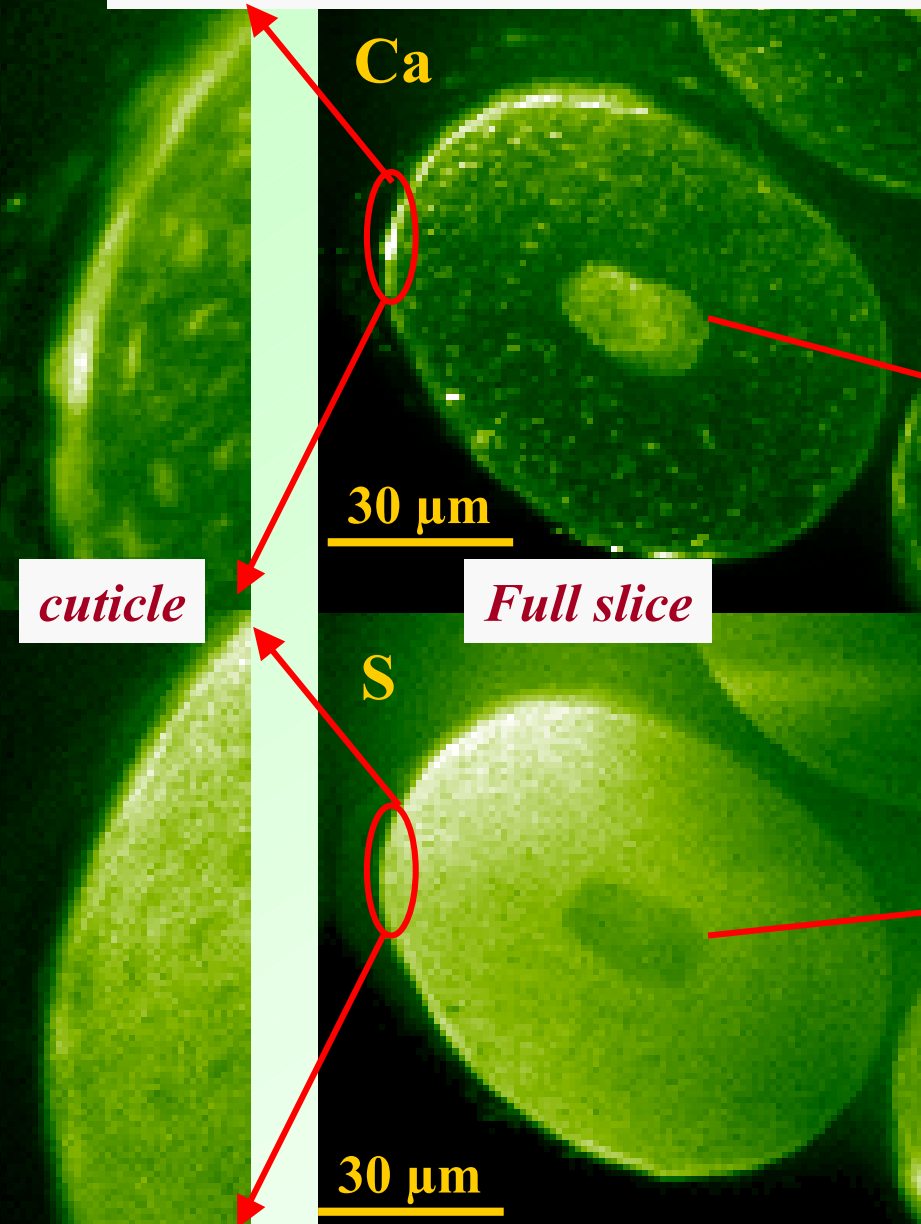
### Needed:

Large number of samples !!!  
Complementary techniques, SAX,  
IR  
Careful sample preparation

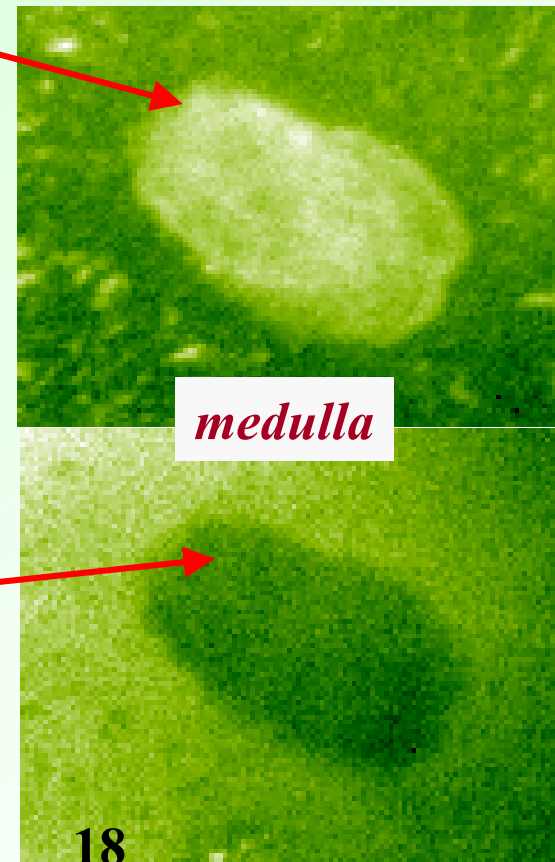


# XRF mapping of hair sections, ID21

C. Mérigoux, F. Briki, L. Kreplak, J. Doucet, LURE, Orsay.  
J. Susini, M. Salomé, ESRF-ID21, Grenoble.



- Excitation Energy: 4.1keV
- Probe size:  $0.20 \times 0.24 \mu\text{m}^2$
- 100ms/pixel



# Scanning micro-XRF, biological applications

## Single cell spectroscopy

S. Bohic, A. Simionovici, ESRF, Ortega R - Devès G. , CNRS, Bordeaux CNRS Bordeaux,  
Medical beamline, IBS, CHU-G

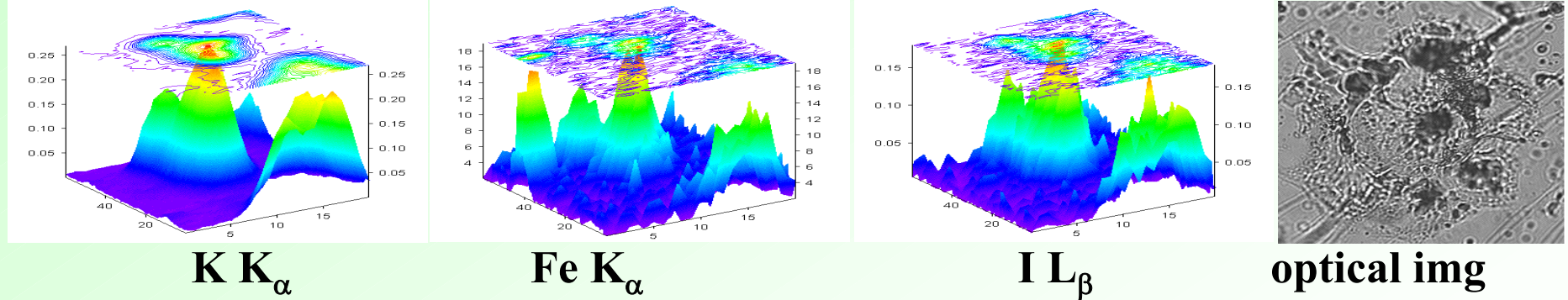
**Aim:** study of the

- biological effects
- intracellular distribution
- anticancer action

anticancer drugs:  
  
low 1 mg/ml conc.

of various high Z labelled anticancer drugs used at pharmacological doses

Ovarian cancer cell



PINK beam:  $1 \times 5 \mu\text{m}$  (min), flux  $\geq 5 \cdot 10^{11} \text{ ph/s}$ , CRL lenses

Non-destructive: dry or freeze-dry samples,  $t \leq 5 \mu\text{m}$

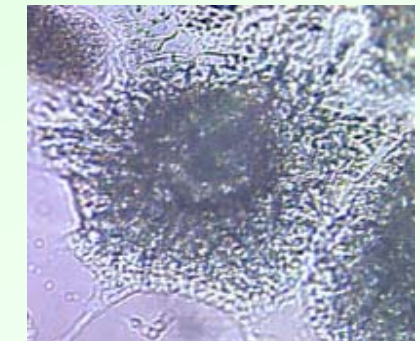
Mapping: 2-4 hours, 1-2 sec./point (PINK),  
 $t > 20\text{h}$  (monochromatic)

# Scanning micro-XRF, biological applications

## Intracellular distribution of $\text{GaNO}_3$

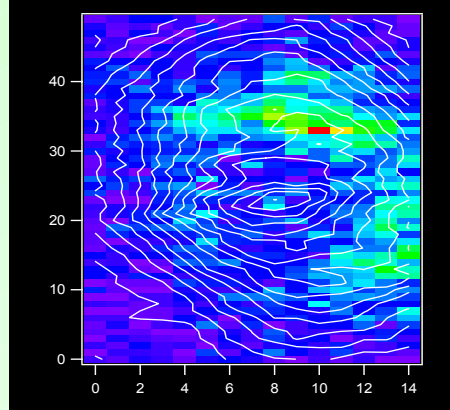
Ortega R - Devès G. , CNRS, Bordeaux ---- ID22: S. Bohic, A Simionovici

- 250 mM Gallium nitrate – 48 H ,  $\Leftrightarrow$  50% inhibition growth
- Cells grown as monolayer- cryofixed & lyophilized.
- $E = 14 \text{ KeV}$ , beam size  $2 \times 10 \mu\text{m}^2$ , Flux= $2.10^{10} \text{ ph/s}$ , in air
- Al-Compound Refractive lenses (CRL)
- Dim.  $50 \times 60 \mu\text{m}^2$ , 5 sec/points, pixel  $1 \times 4 \mu\text{m}^2$

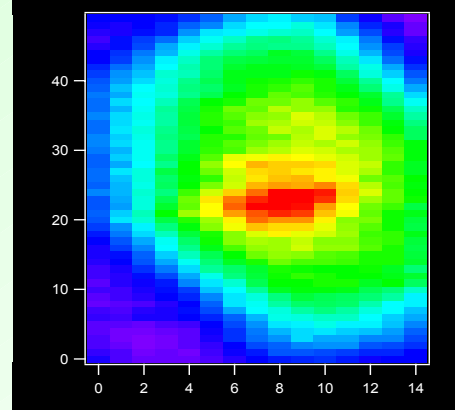


Ga : average of  $40 \mu\text{g/g}$  dry mass

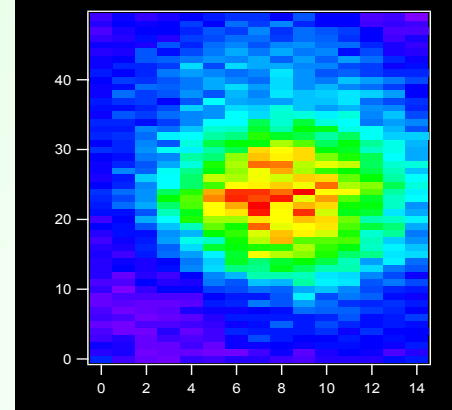
Fe- $K_\alpha$



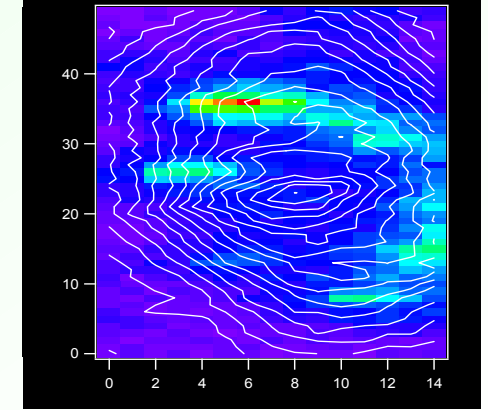
K- $K_\alpha$



Zn- $K_\alpha$



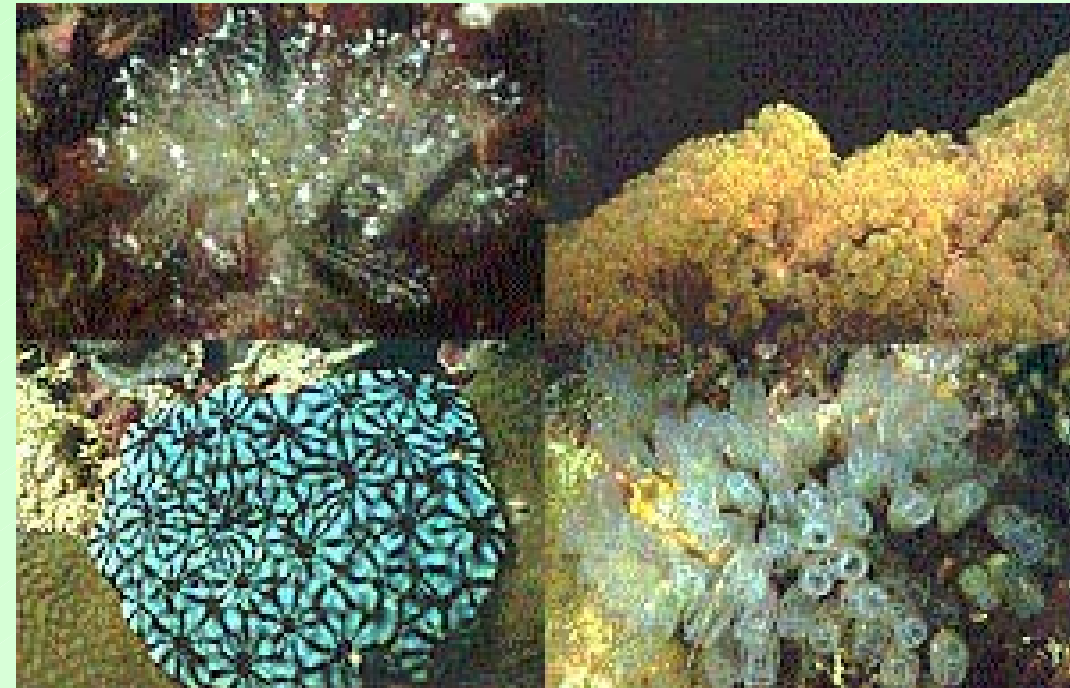
Ga- $K_\alpha$



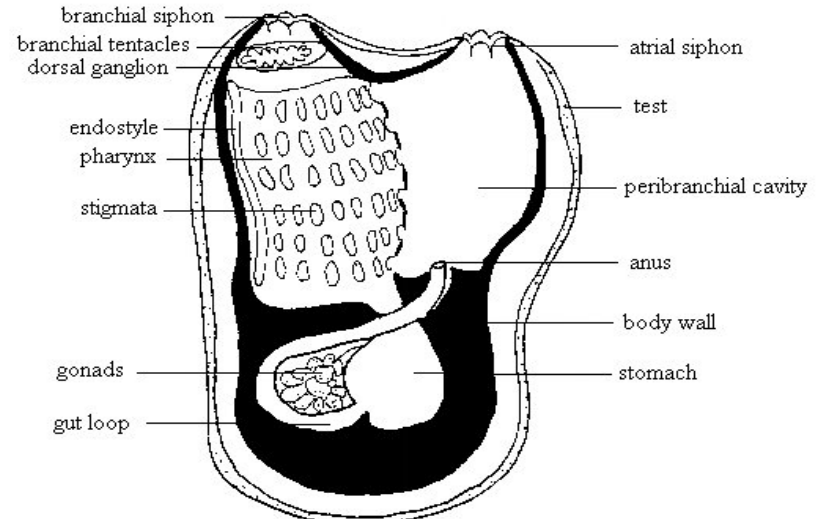
- Localisation of the gallium in small round structures in the perinuclear region - typical of lysosomal material

# Scanning micro-XRF, biological applications

## Vanadium accumulation in Ascidiants (sea squirts or tunicates)



Anatomy of a basic ascidian (Aplousobranch type)



M. Henze, Z. Physiol Chem, 72, 1911  
H. Michibata *et al.*, "Vanadium in the environment, Part 1", 1998

### Averaged Vanadium concentration:

Sea water:	$\sim 3.5 \cdot 10^{-8} \text{ mol/dm}^3$
<i>Ascidian Gemmata:</i>	$\sim 3.7 \cdot 10^{-1} \text{ mol/dm}^3$
<i>Ascidian Syndneisis :</i>	$\sim 1.3 \cdot 10^{-2} \text{ mol/dm}^3$

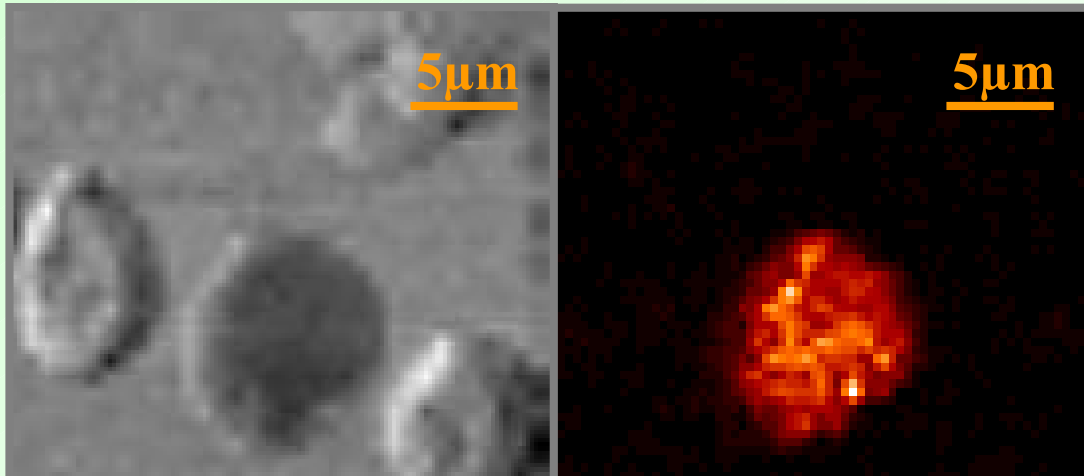
# Vanadium accumulation in Ascidians (sea squirts or tunicates)

## DIC+Fluorescence on living cells: identification of true vanadocytes, ID21

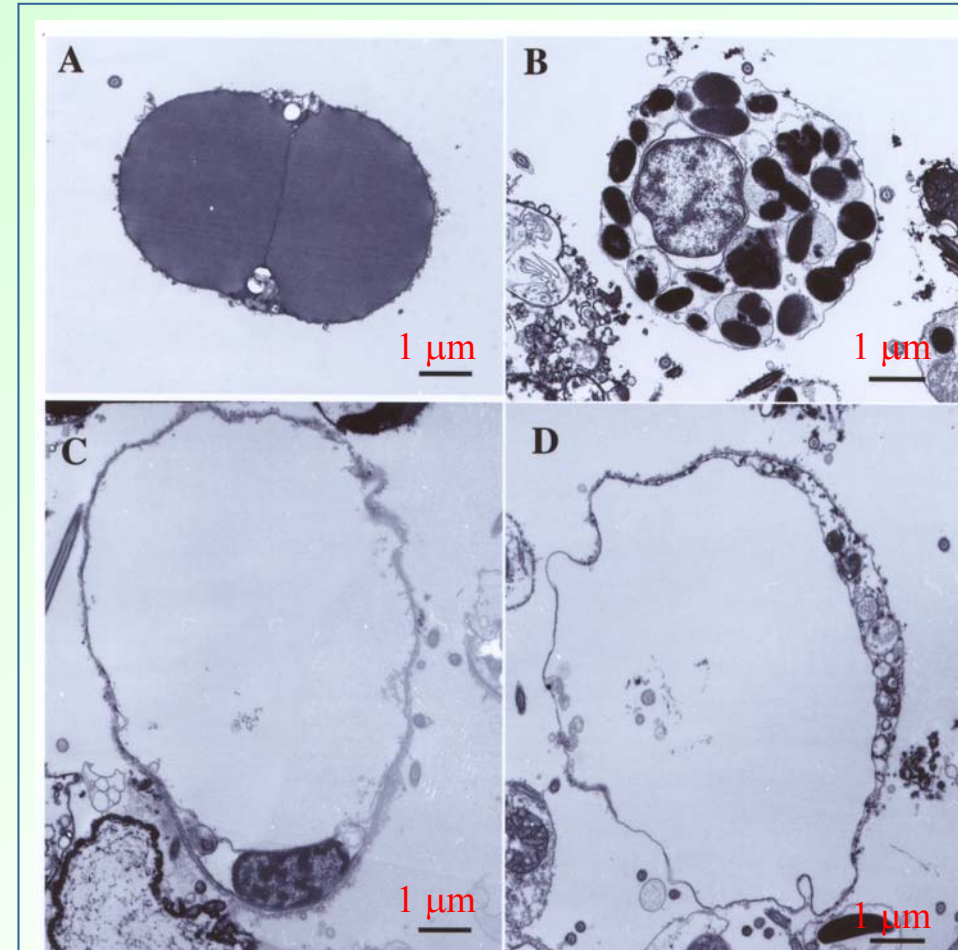
- ✓ 9 to 11 different types of blood cells.
- ✓ Identification of true vanadocytes is still a subject of controversy.

- ✓ Excitation energy: 5.5 keV
- ✓ Probe size: 0.3x0.3 $\mu\text{m}^2$
- ✓ Dwell time: 0.1 s/pixel

Vanadium < 300 ppm



T. Ueki *et al.* *Zoological Science*, **19**, (2002) 22



**Electron micrograph**

*A: compartment cell*

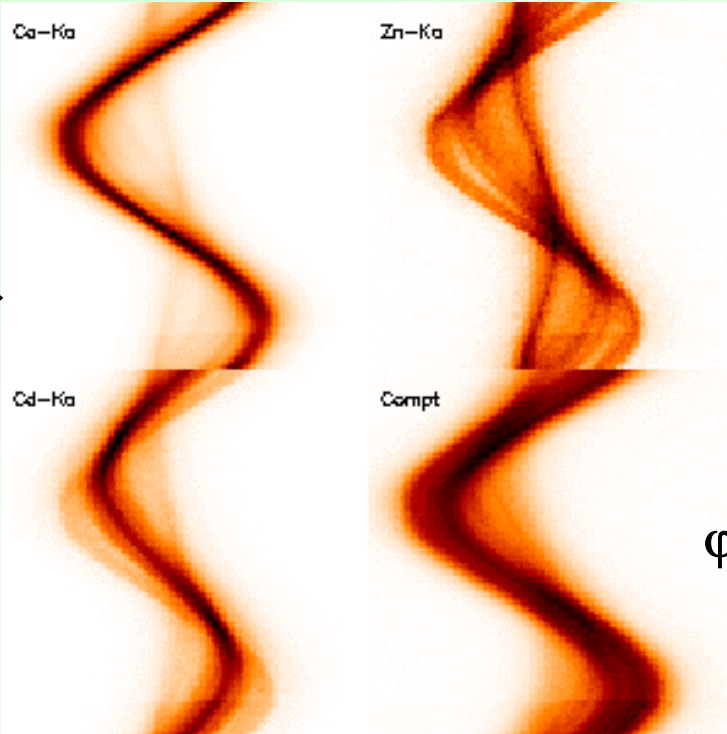
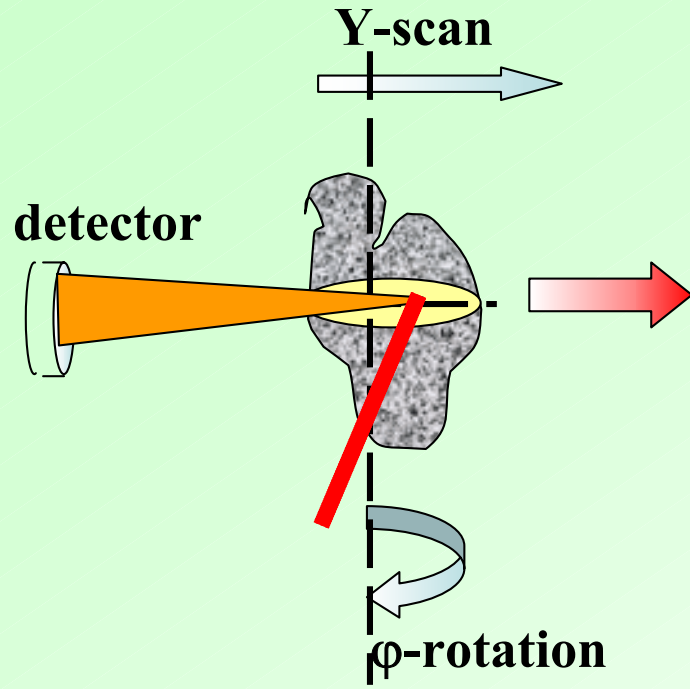
*B: pigment cell*

*C and D: signet ring cell*

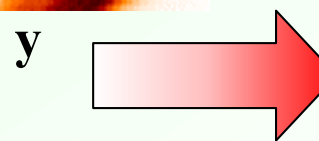
# Scanning micro-XRF, 2D/3D internal elemental distribution

## Fluorescence tomography

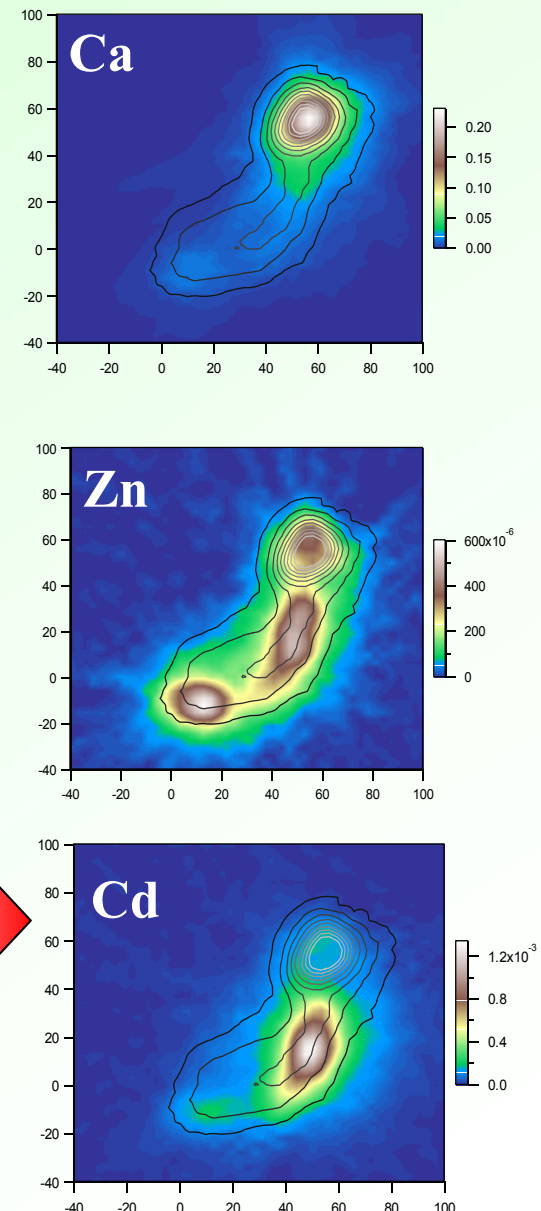
### Sinogram: 2D ( $y - \varphi$ ) intensity map



Several slices: complete  
3D distribution, time-  
consuming



Reconstruction algorithm  
2D, (x-y) internal intensity  
(concentration)  
distribution

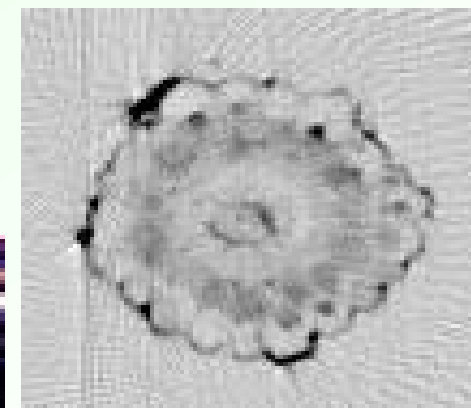
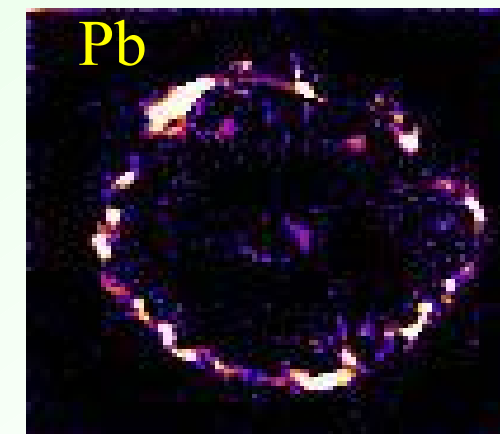
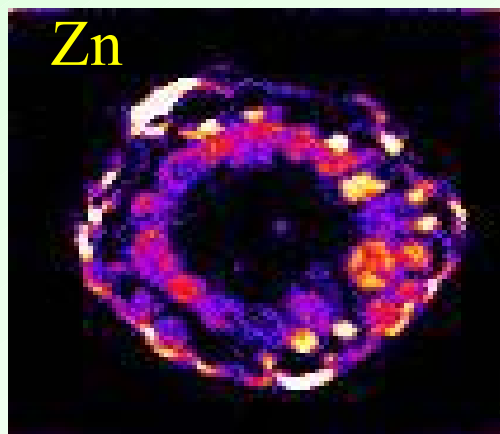
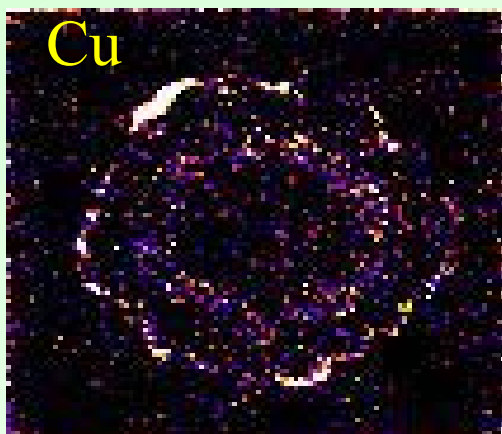
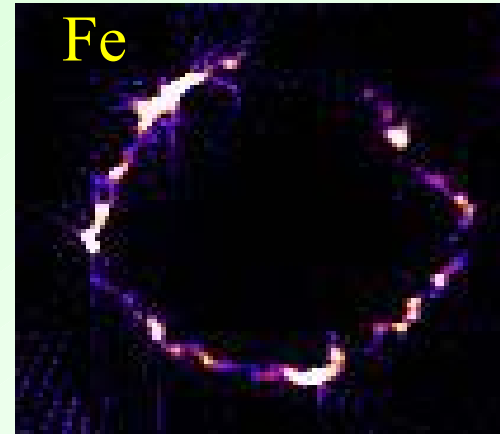
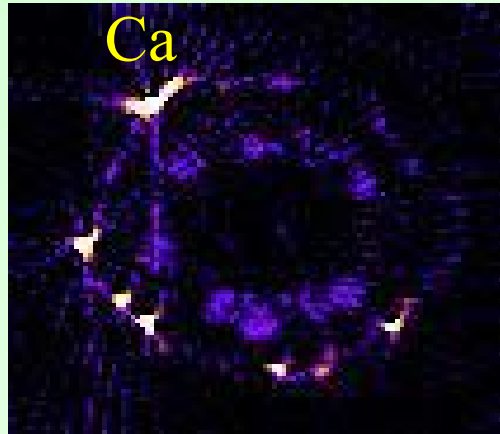
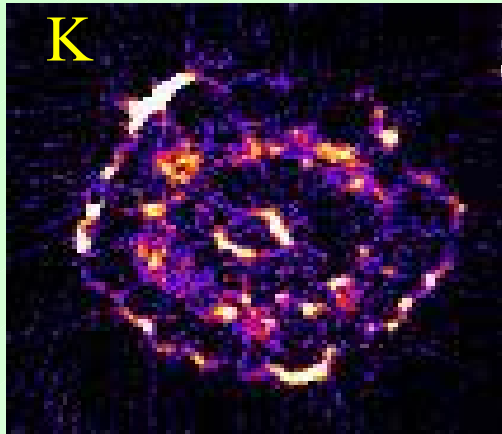


# Fluorescence tomography, biological application

W. Schröder, FZ Julich, Ch. Schroer, T.F. Günzler, B. Lengeler, RWTH  
Aachen, A. Simionovici, CNRS

## Study of ion transport in plants

Mycorrhizal root of tomato plant root -  $\varnothing < 0.5$  mm; resolution  $\approx 1 \mu\text{m}$



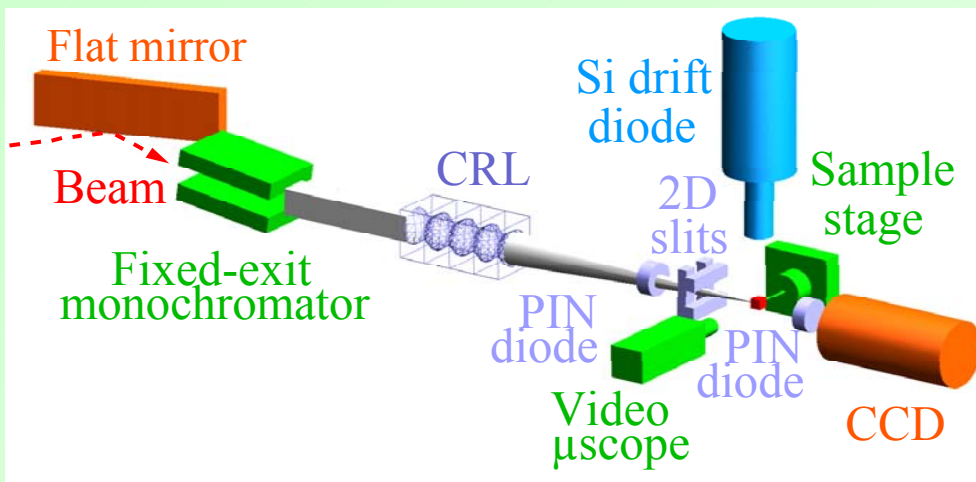
Transmission

# Fluorescence tomography, biological application

## Search for ET life on micro-meteorites

L. Lemelle, Ph. Oger, Ph. Gillet, ENS Lyon, France

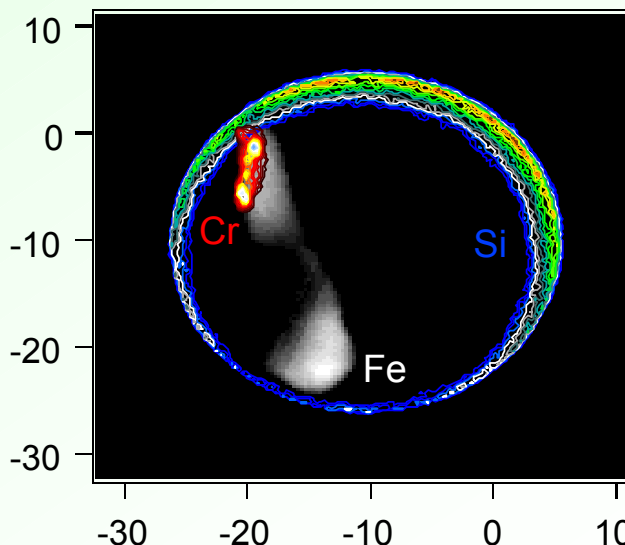
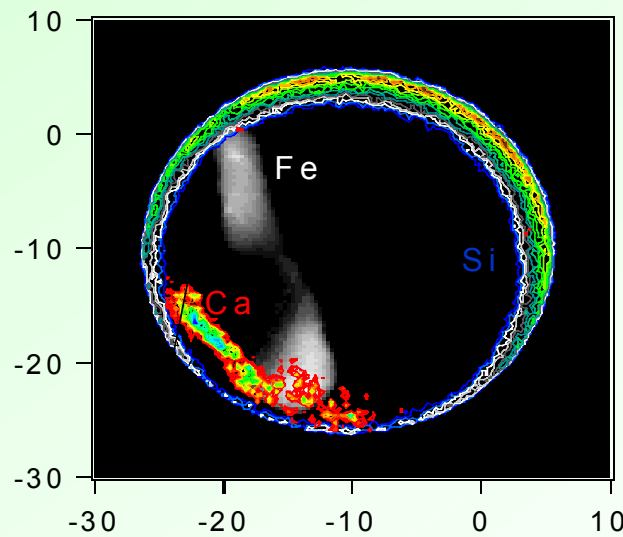
A. Simionovici, M. Chukalina \*, B. Golosio, Ch. Rau, ID22, J. Susini, ID21, ESRF



**Non-destructive imaging of carbonate sites of formation of bacteria-like remnants - on mineral surfaces, w/o contamination**

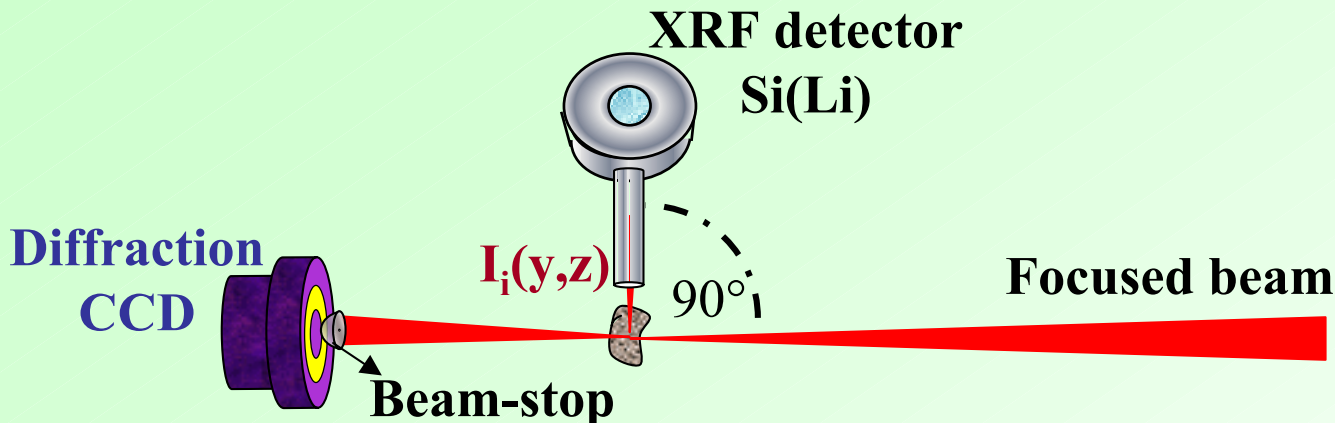
**Complementary to IR, SEM/TEM investigations**

**Preparation for MARS return samples - mini-P4 container**



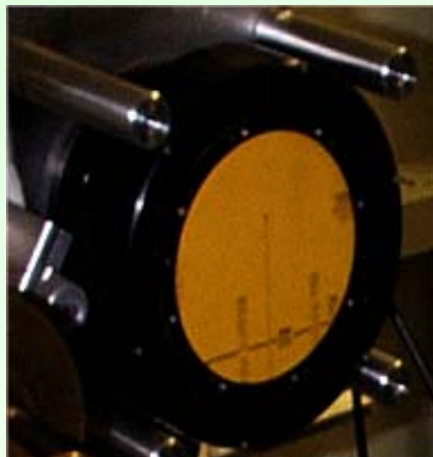
**2  $\mu$ m resolution  
2 s/pixel**

## Scanning $\mu$ -XRF + Combined techniques



2D large area low resolution detector in transmission geometry:

Powder diffraction  
Small angle scattering



Information about the **crystalline structure** of the irradiated **microspot**

**simultaneously** with micro-XRF



Simultaneous XRF+XRD mapping

# Scanning $\mu$ -XRF + $\mu$ - XRD

## Effect of Sr to the evaluation and structure of bone

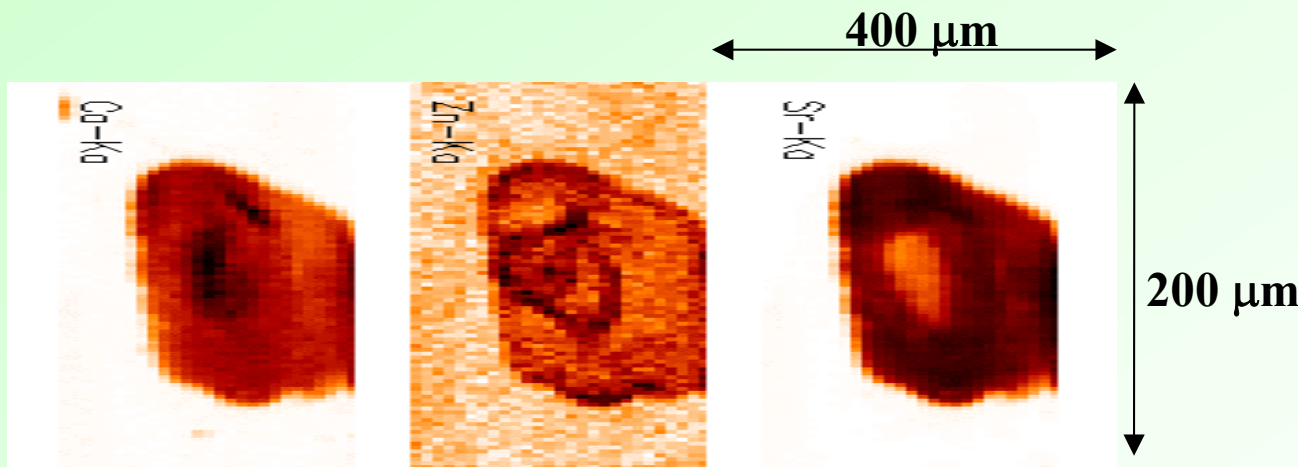
In collaboration: S.C. Verberckmoes, G.J. Behets, A. R. Bervoets, L. Oste, M. E. De Broe, P. C. D'Haese, Dep. of Nephrology-Hypertension, Univ of Antwerp, K. Janssens, Dep of Chemistry , Univ of Antwerp, Belgium, S. Bohic, ID22, ESRF, France

### Background :

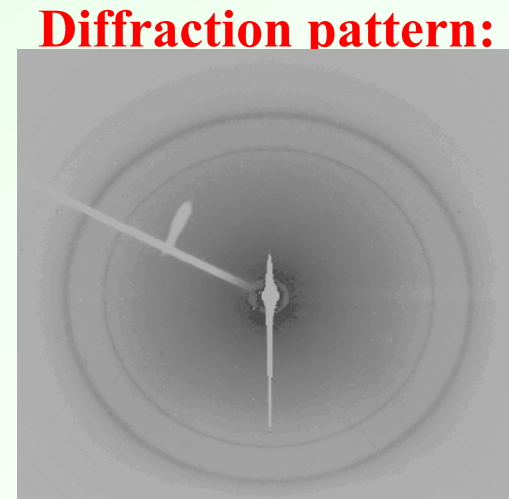
- Sr accumulation in bone from dialysis patients of renal failure?

### Aim of the study:

- Localization of Sr
- Does Sr alter the bone mineral ? How? Why?



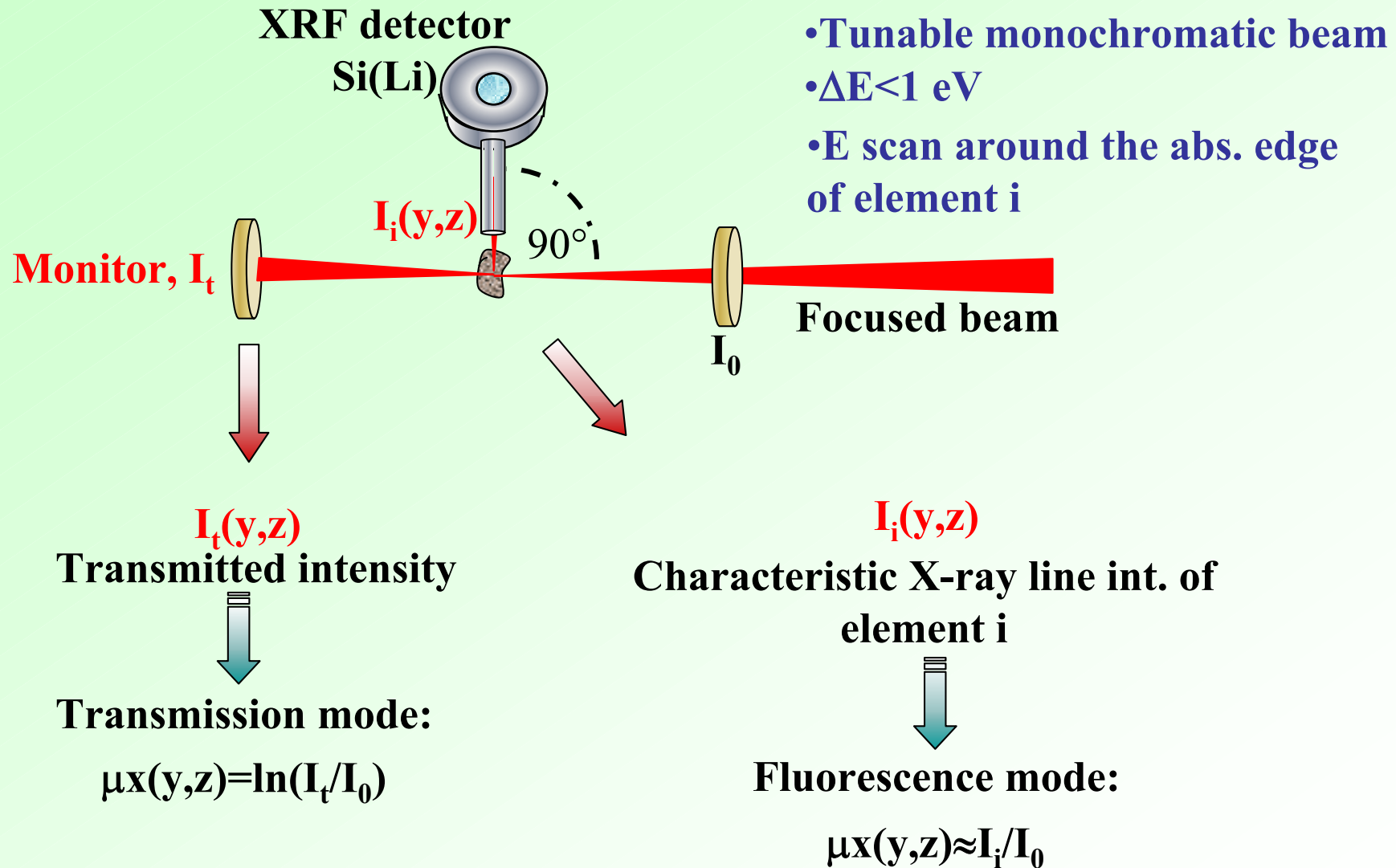
XRF elemental maps of trabecular bone



Diffraction pattern:  
Information about crystallinity

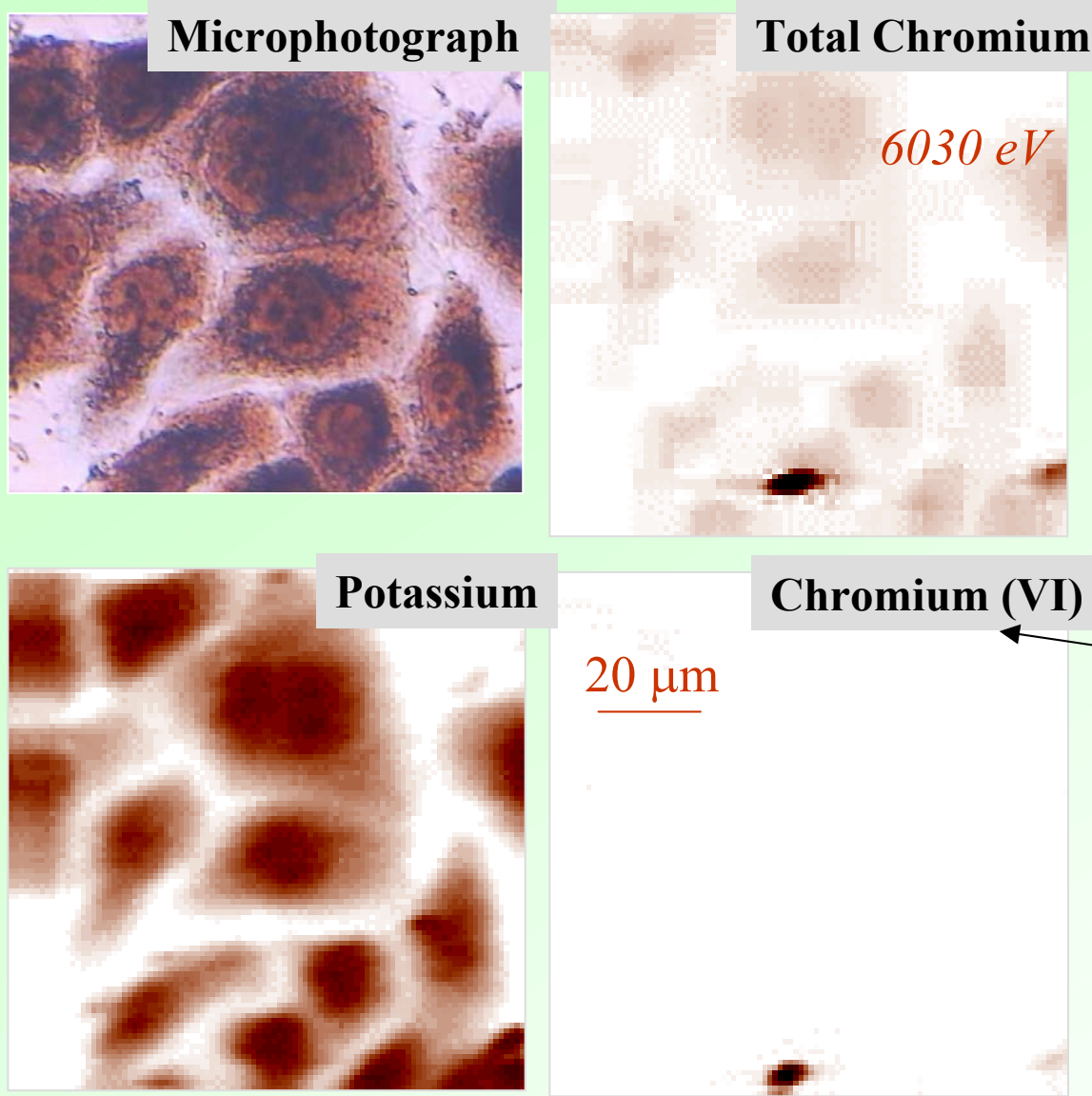
- $10 \mu\text{m}$  thick bone section of rats suffering from chronic renal failure induced by 12 weeks daily oral dose ( $0.3\text{g Sr}/100\text{ml water}$ ) -> induced osteomalacia.
- E: 17 keV, spot-size, VxH:  $2 \times 15 \mu\text{m}^2$ , LT: 2 s/pixel, CRL of 56 lenses

## Scanning $\mu$ -XRF + Combined techniques

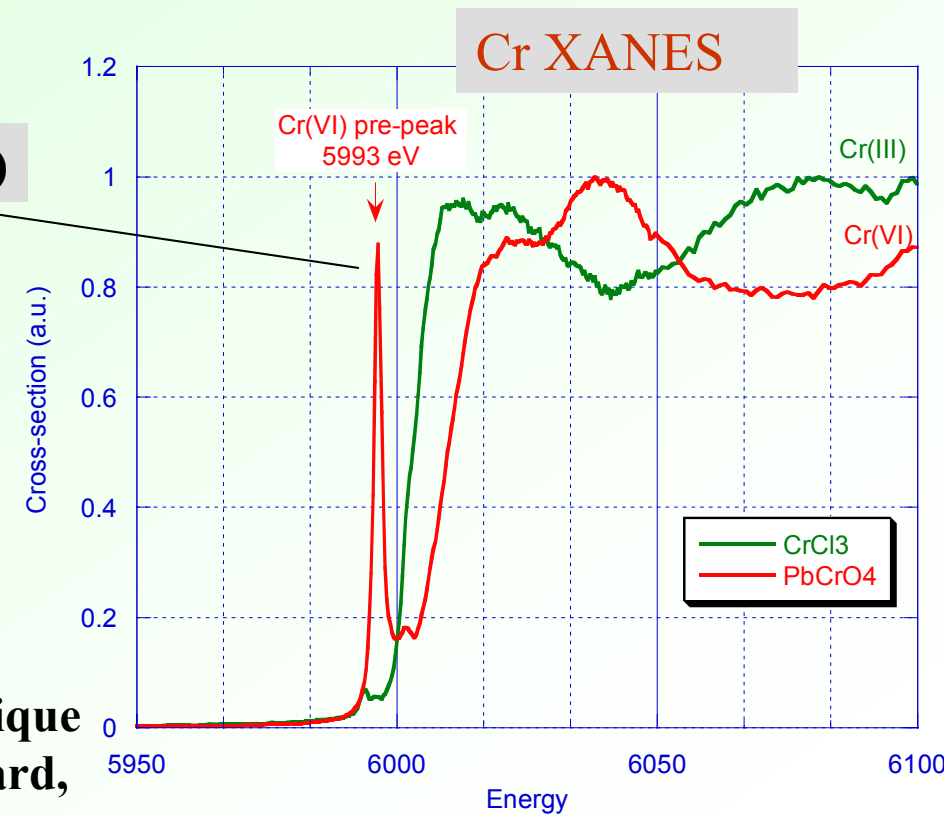


Information about chemical speciation of the micro-spot,  $\mu$ -XAS

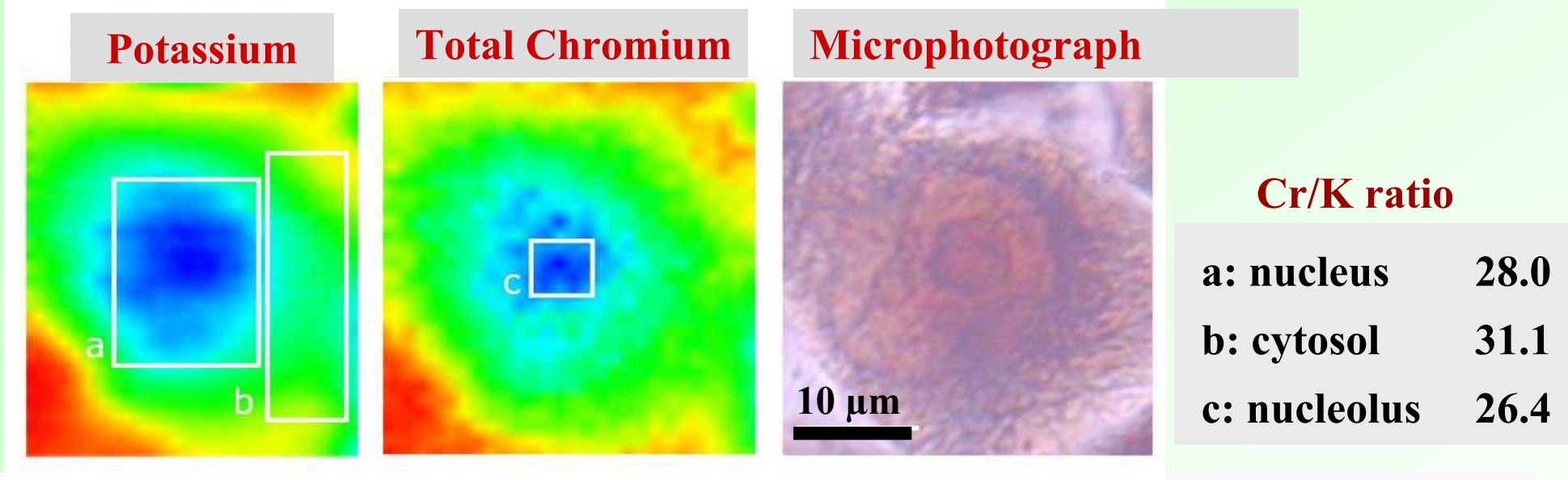
# Chemical mapping: chromium oxidation states in single-cells



- Human ovarian cells exposed in vitro to 1 µg/ml  $\text{PbCrO}_4$
- Freeze-dried sample
- X-ray microprobe size : 1 x 3  $\mu\text{m}^2$
- Field of view : 100  $\mu\text{m}$  x 100  $\mu\text{m}$



## Chemical mapping: chromium oxidation states in single-cells



- Cell exposure to low solubility ( $\text{PbCrO}_4$ ), and soluble ( $\text{Na}_2\text{CrO}_4$ ), Cr(VI) compounds results in intracellular accumulation of reduced forms of Cr.
- Reduced forms of Cr are homogeneously distributed within the cell volume, including the cell nucleus.
- Cr(VI) was observed in the cell environment (aggregates) only after  $\text{PbCrO}_4$  exposure
- The stronger carcinogenicity of low solubility chromate compounds vs soluble compounds may derived from the combinative genotoxic effects of intracellular Cr (DNA bound ?) and long term exposure to a strong oxidant, Cr(VI).

# Scanning $\mu$ -XRF + Combined techniques

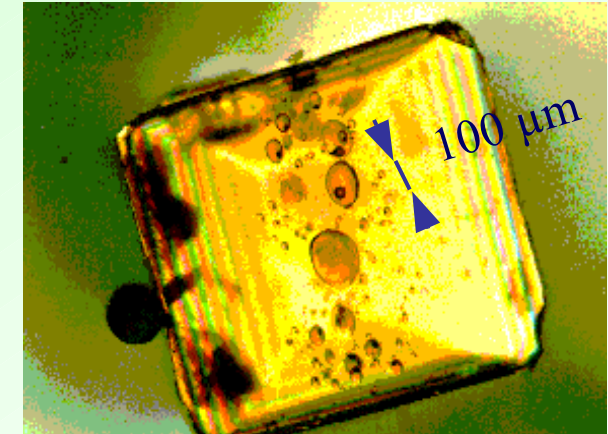
## Speciation of Fe in silicate glasses by $\mu$ -Xanes

M. Bonnin, N. Métrich, JP Duraud, CEA, Paris, A. Simionovici, ID22, CNRS

**Redox states of Fe/S - control mineralogical phases of magma**

- fluid inclusions are magma depth witnesses ( $1100 - 1300^\circ$ )
- S degassing - environmental key parameter (Stromboli: 800 t/day)

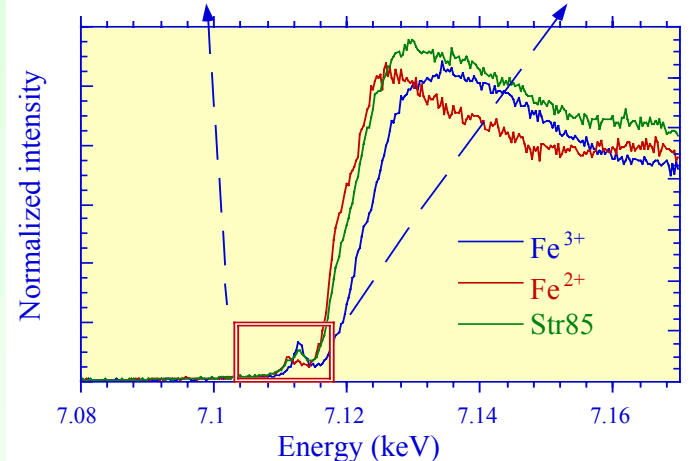
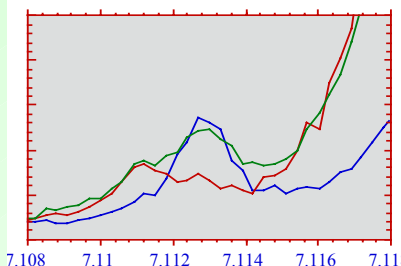
- spatial distribution of  $\text{Fe}^{2+,3+}$
- ref. point for oxidation state
- pre-peak serves as quant. par. for  $\text{Fe}^{3+}/\text{S}$  Fe



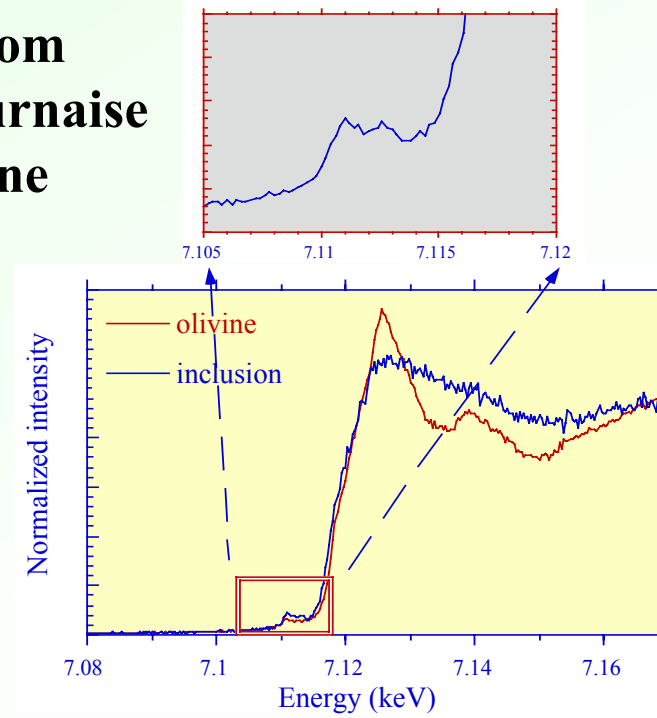
**Glass standards  
containing Fe**

Lava melts at  $1300^\circ\text{C}$

Close to glass inclusions



**Inclusion from  
Piton de la Fournaise  
Host: olivine**



# **Scanning $\mu$ -XRF + Combined techniques**

## **Environmental application, investigation of single fly ash particles**

In collaboration: C.M. Camerani, B.M. Steenari, O. Lindquist Chalmers Univ. , Göteborg, Sweden,  
B. Golosio, S. Ansell, A. Simionovici, ID22

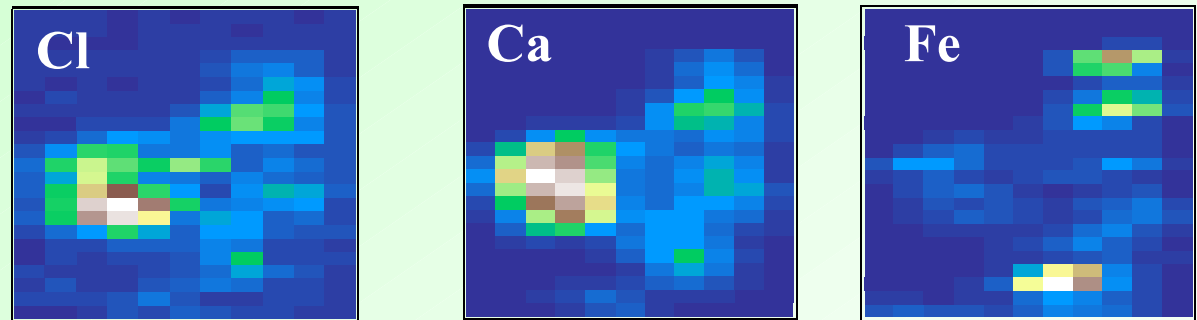
### **Aim of the study:**

- During combustion large amount of fly ash is created
  - Fly ash is a potential danger for the environment
  -
- Prediction of the short and long term fate of heavy metals in fly ash particles
- Influence of the chemical speciation of the different elements, crystal structure and porosity of the matrix on the weathering rate
- Toxicity depends on the elemental concentration and speciation

# Scanning $\mu$ -XRF + Combined techniques

## Environmental application, investigation of individual fly ash particles

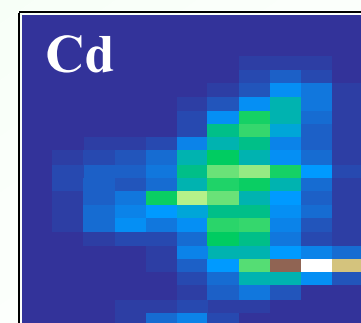
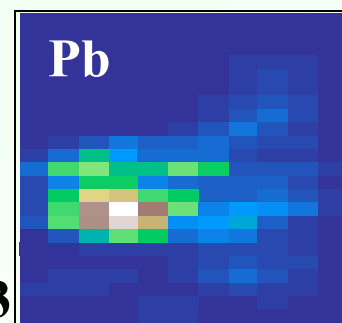
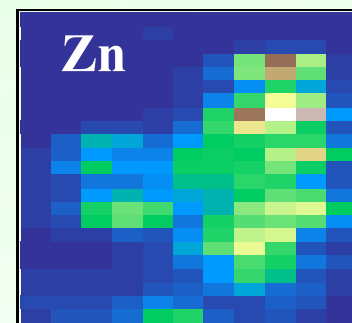
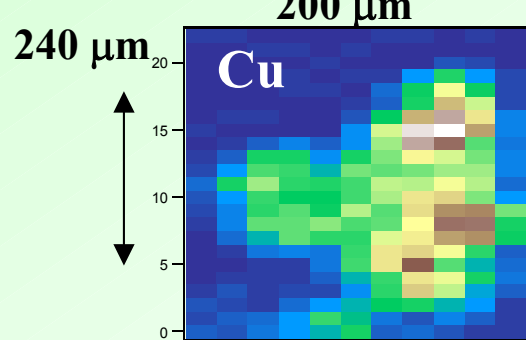
In collaboration: C.M. Camerani, B.M. Steenari, O. Lindquist Chalmers Univ. of Techn., Göteborg, Sweden, B. Golosio, A. Simionovici, ID22



scanning=2D projection of a 3D object!

Intensity distribution reflects the concentration and topological change within the sample

XRF tomography: internal elemental distribution within e.g. slice1 and slice2

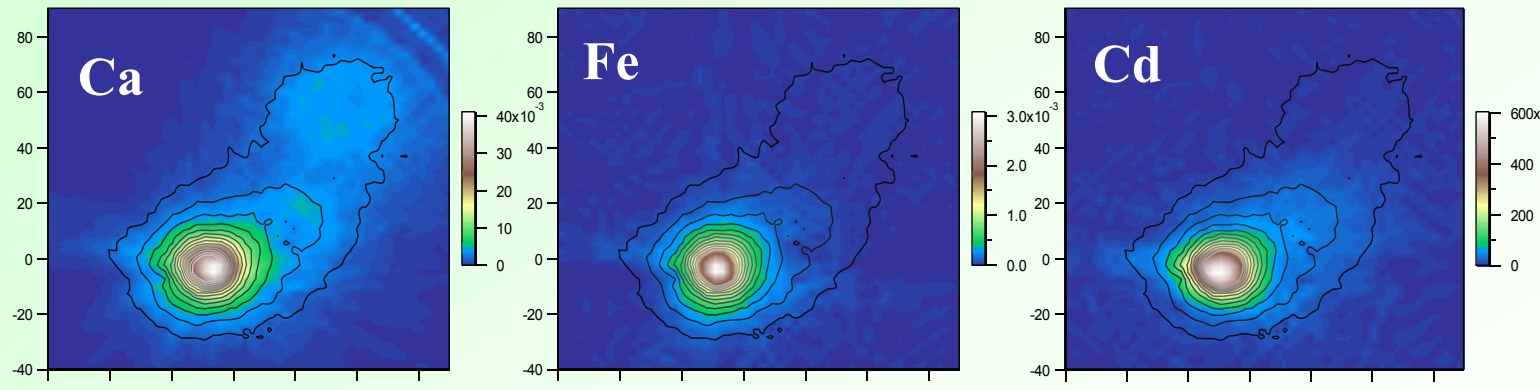


# Scanning $\mu$ -XRF + Combined techniques

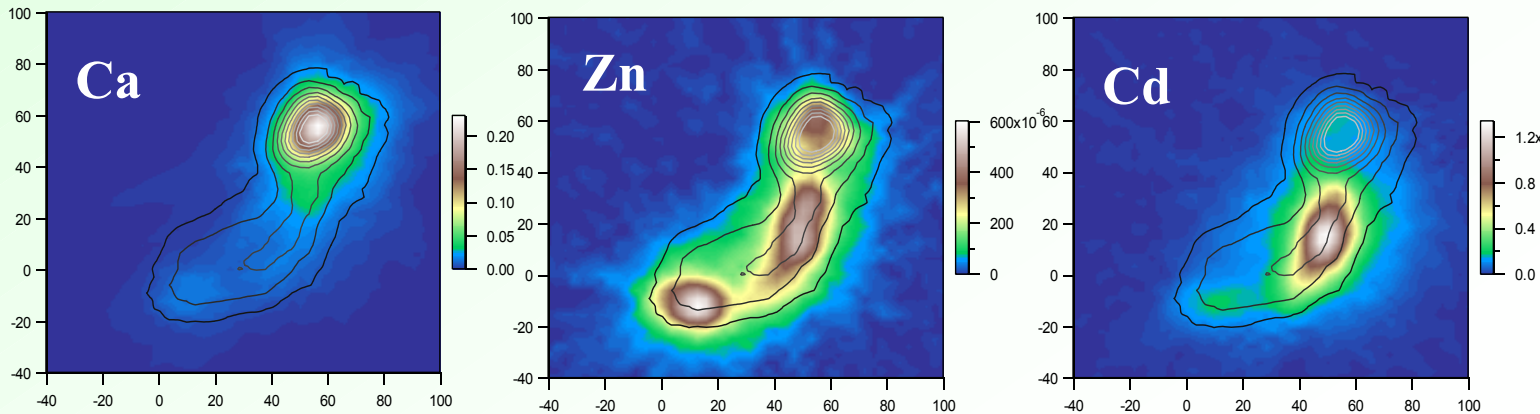
## Environmental application, investigation of individual fly ash particles

In collaboration: C.M. Camerani, B.M. Steenari, O. Lindquist Chalmers Univ. of Techn., Göteborg, Sweden, B. Golosio, A. Simionovici, ID22

Internal elemental distribution within Slice2



Internal elemental distribution within Slice1



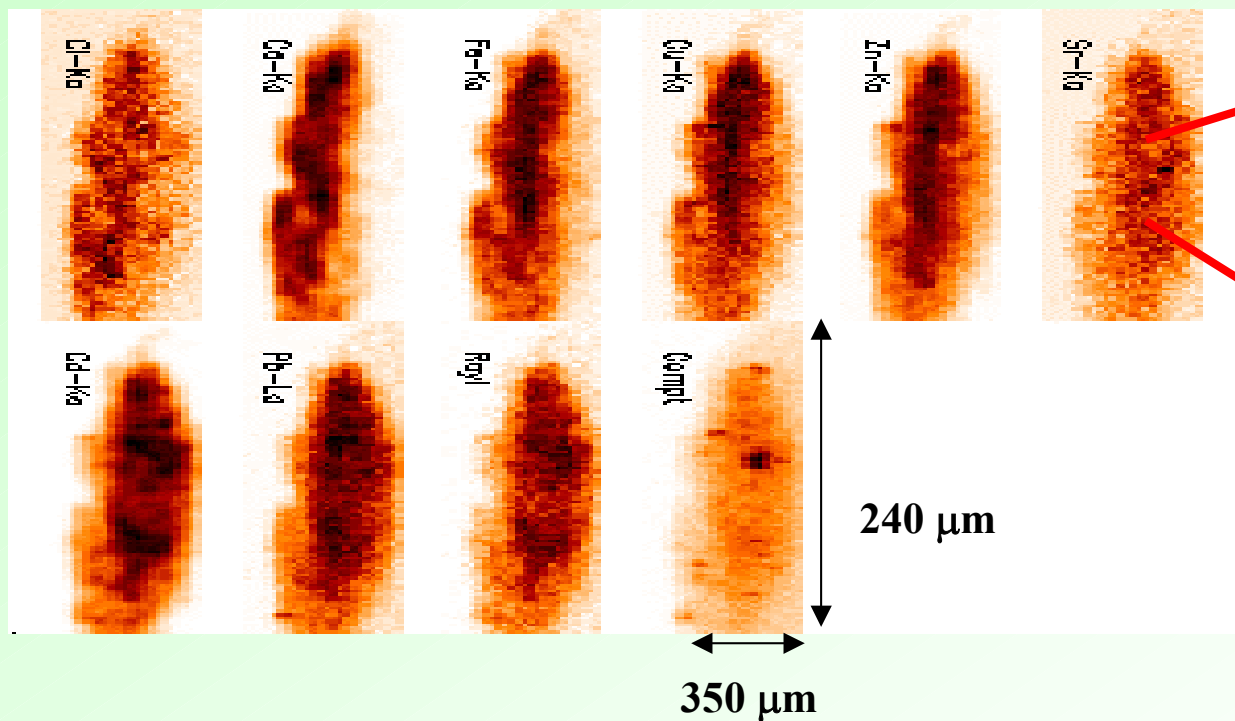
# Scanning $\mu$ -XRF + Combined techniques

## Environmental application, investigation of individual fly ash particles

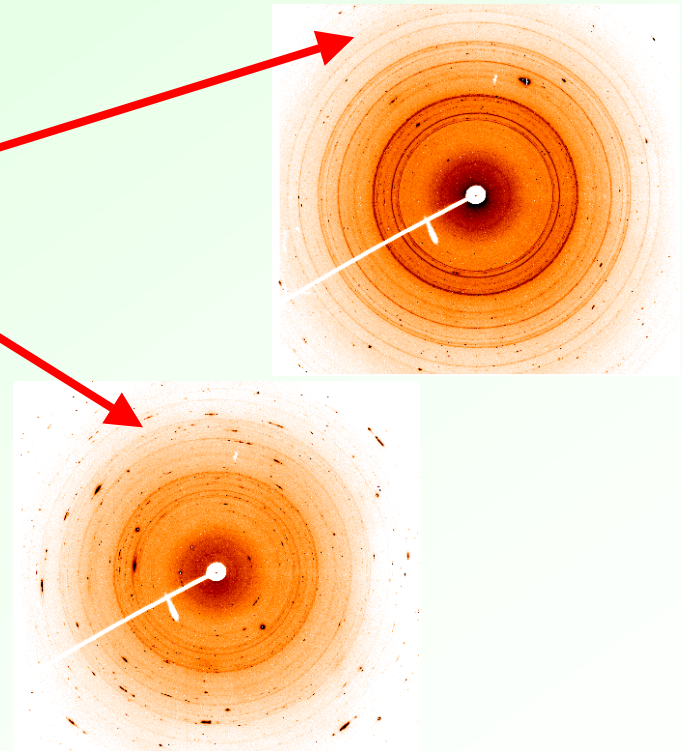
In collaboration: C.M. Camerani, B.M. Steenari, O. Lindquist Chalmers Univ., Göteborg, Sweden,  
B. Golosio, S. Ansell, A. Simionovici, ID22

### Crystalline structure: micro-XRD

Scanning-Micro-XRF



Micro-XRD

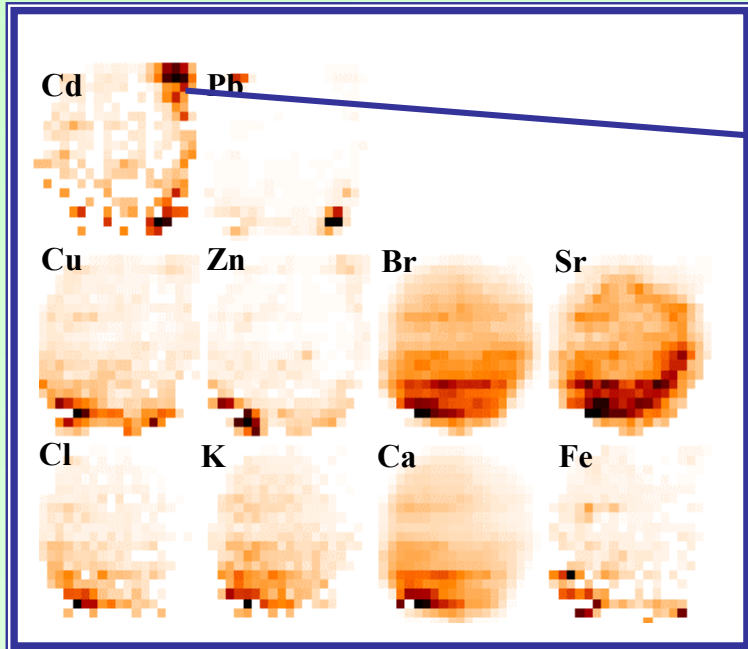


Single waste fly ash particles, LT:6 s, step-size H\*V:14\*3  $\mu\text{m}^2$ , ID18F/ID22  
35

# Scanning $\mu$ -XRF + Combined techniques

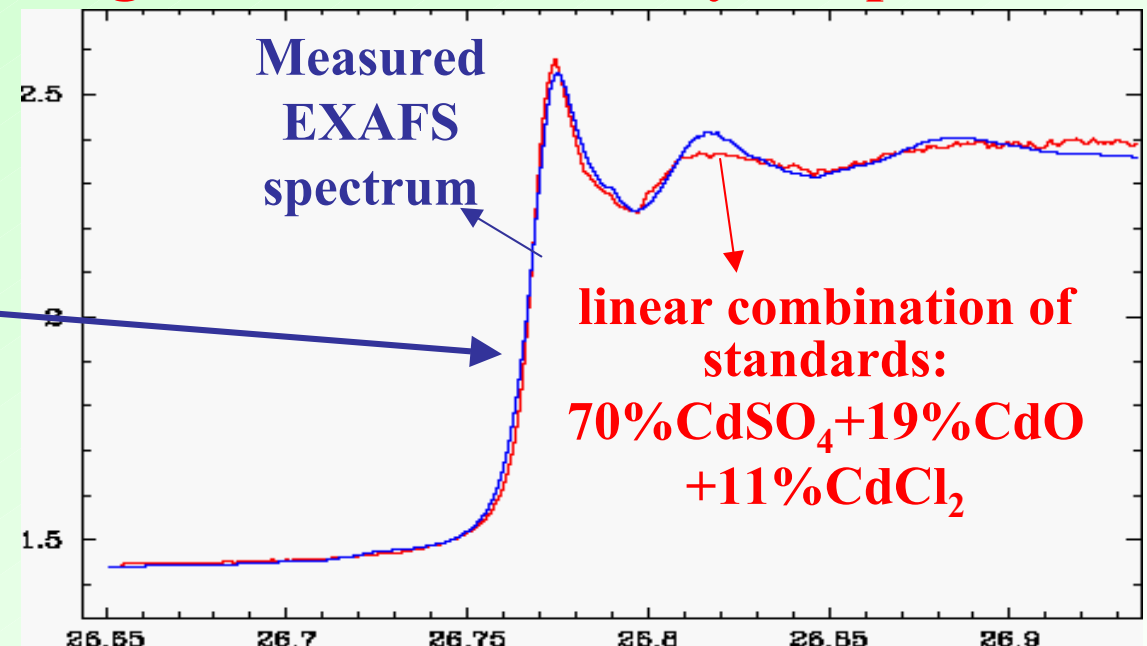
## Environmental application, investigation of individual fly ash particles

### Scanning- $\mu$ -XRF

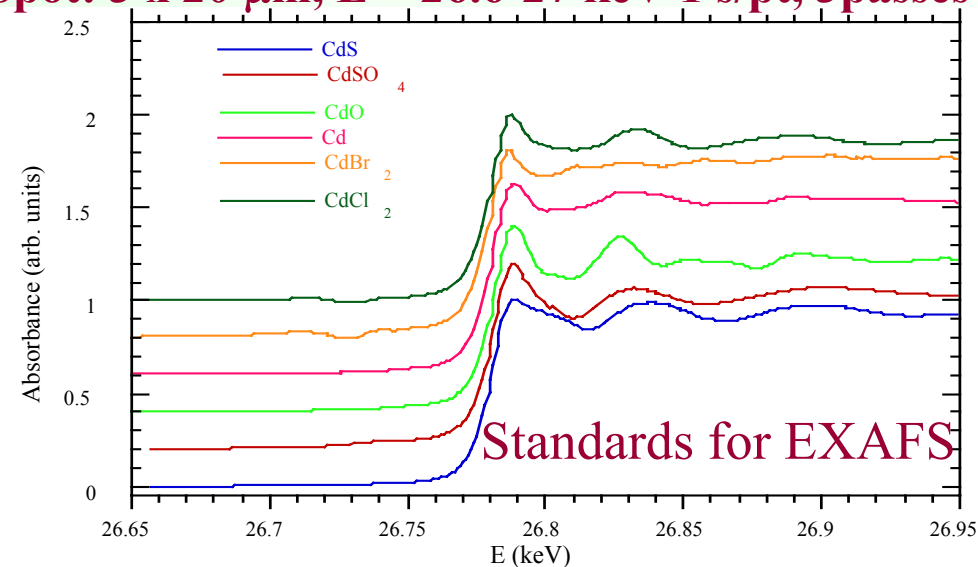


Spot:  $8 \times 8 \mu\text{m}^2$ , E = 27 keV, LT: 6 s/pt

Chemical speciation and coordination number  
of Cd in the chosen pixel:  $\mu$ -EXAFS



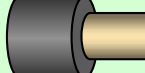
Spot:  $3 \times 20 \mu\text{m}$ , E = 26.6-27 keV 1 s/pt, 3 passes



# Scanning $\mu$ -XRF + Combined techniques

High resolution

CCD

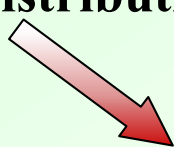


- Full ( $1 \times 1 \text{ mm}^2$ ) beam

High resolution CCD:

- absorption (phase contrast) imaging

- absorption tomography: 3D linear absorption coefficient distribution



- Dual energy tomography: 3D elemental distribution of a chosen element

- XANES imaging: stack of absorption images around the abs. edge of a given element

- Tunable monochromatic beam
- $\Delta E < 1 \text{ eV}$
- E scan around the abs. edge of element i



# Study of Chernobyl hot-spots

In collaboration with B. Salbu, O. C. Lind, T. Krekling, Agricultural Univ. of Norway, Norway  
K. Janssens, L. Gijsels, Univ of Antwerp, Belgium  
A.Simionovici, CNRS

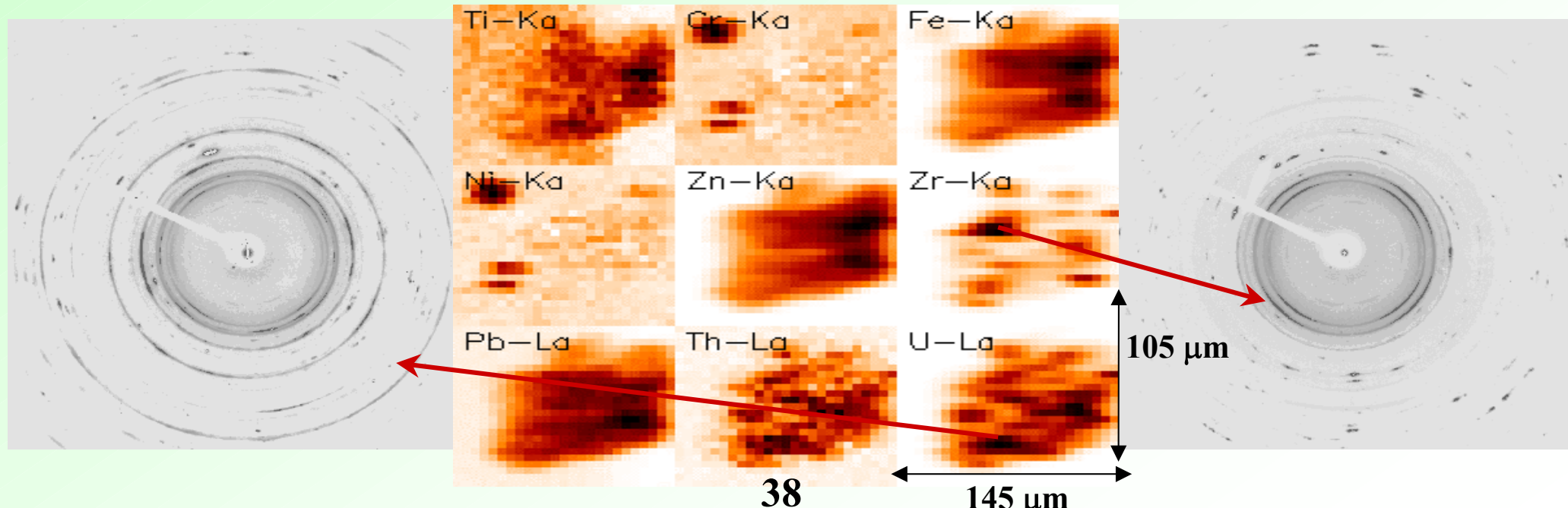
## Background:

- 1986 Chernobyl accident
- Release of high amount of radioactive fuel particles

## Aim of the study:

- Prediction of the short and long term consequences in the environment
- Influence of the oxidation state of U, that of the crystal structure and porosity of the particles on their weathering rate

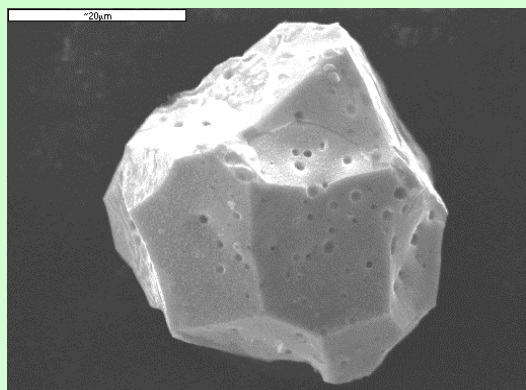
Individual particle, E: 28 keV, spot HxV:  $2 \times 5 \mu\text{m}^2$ , LT: 20 s/pixel, **simultaneous XRF+XRD mapping**,  
CRL of 140 lenses, ID18F



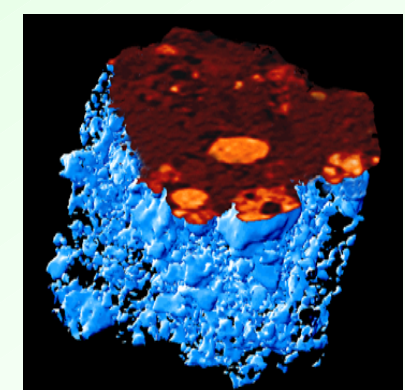
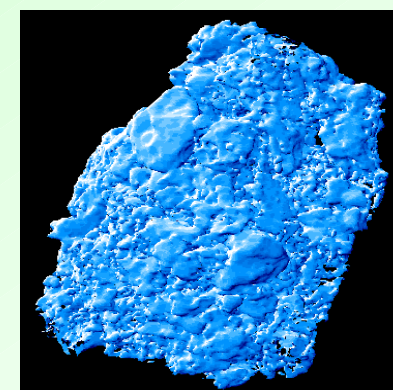
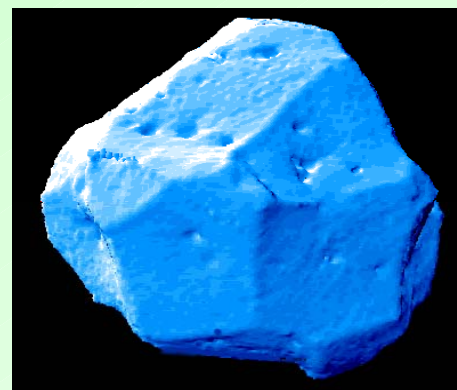
# Study of Chernobyl hot-spots

B. Salbu, O. C. Lind, T. Krekling, Agricultural Univ. of Norway, Norway, K. Janssens, Univ of Antwerp, Belgium, A.Simionovici, CNRS, Lyon, France, C. Rau, ESRF, Grenoble, France

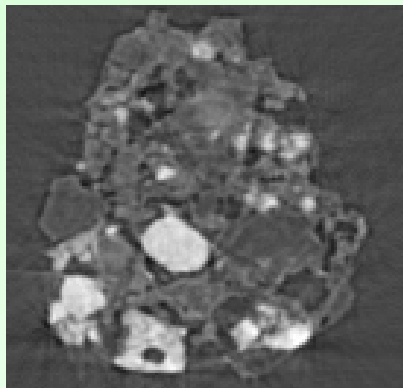
SEM Image



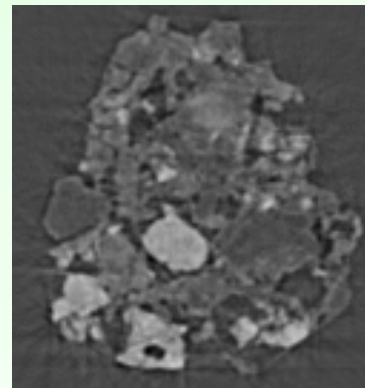
absorption tomography, 1  $\mu\text{m}$  res.,  $E = 20 \text{ keV}$



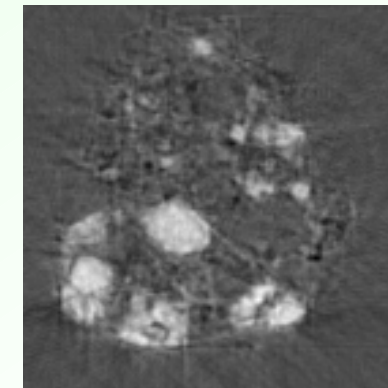
Dual energy absorption tomography: 3D distribution of a given element



$E \approx 17.2 \text{ keV}$



$E \approx 17.1 \text{ keV}$



Difference

# Study of Chernobyl hot-spots

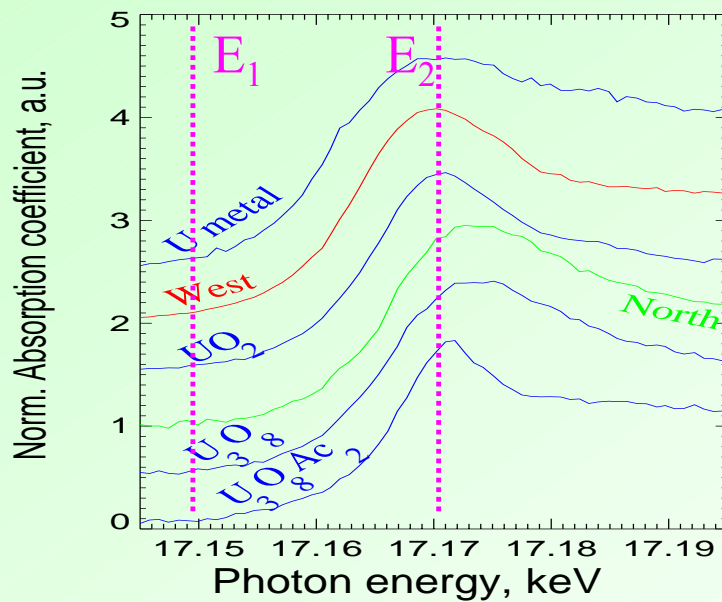
B. Salbu, O. C. Lind, T. Krekling, Agricultural Univ. of Norway, Norway, K. Janssens, Univ of Antwerp, Belgium, A.Simionovici, CNRS, Lyon, France, C. Rau, ESRF, Grenoble, France

## $\mu$ -chemical speciation of uranium

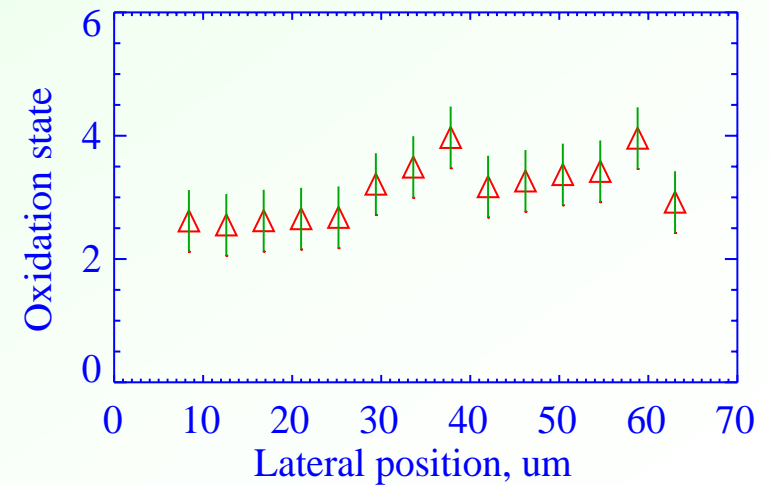
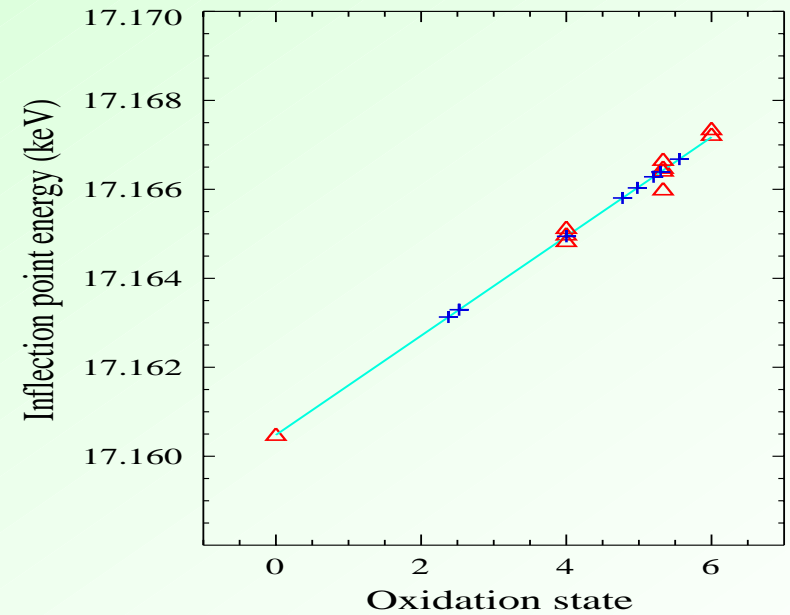
calibration: U metal,  $\text{UO}_2$  and  $\text{U}_3\text{O}_8$  ( $0^+ - 6^+$ )

$\text{FWHM} \geq 0.15 \text{ eV}$ ,  $dE \approx 0.8 \text{ eV/q}$

$2 \times 5 \mu\text{m}$ , flux  $8 \cdot 10^8 \text{ ph/s.}$ , 2 - 5 sec./point



L<sub>III</sub>-edge  $\mu$ -xanes line scan  
across a particle



## Conclusion

- Scanning micro-XRF analysis is a powerful method of investigation in different research fields, such as biology, environmental science, geology
- It gives information about the 2D elemental distribution and possible correlation among different element
- 2D non-destructive internal analysis: fluorescence tomography
- The combination of different micro-techniques provides more complete information about the sample, e.g. elemental composition, speciation, morphology, crystal structure

# **ID21, ID22/ID18F beam-lines of the ESRF**

**responsible:  
Scientist:**

**BLOM**

**Post. Doc.**

**PhD student:  
Techitian:**

**Visiting  
scientist:**

**ID21**

**M. Salome**

**J. Susini**

**R. Toucoulou**

**U. Neuhaussler  
O. Dhez**

**R. Baker**

**B. Fayard (CNRS)**

**ID22**

**A. Somogyi  
S. Bohic (ID18F)  
M. Drakopoulos (ID18F)**

**B. Golosio  
S. Labouré**

**A. Simionovici (CNRS)**